DESIGN OF UTR-10 FISSION PLATE

by

Seymour John Raffety

A Dissertation Submitted to the

Graduate Faculty in Partial Fulfillment of

The Requirements for the Degree of

DOCTOR OF PHILOSOPHY

Major Subject: Nuclear Engineering

Approved:

Signature was redacted for privacy.

In Charge of Major Work

Signature was redacted for privacy.

Head of Major Department

Signature was redacted for privacy.

Dean of Graduate College

Iowa State University
Of Science and Technology
Ames, Iowa

1964

TABLE OF CONTENTS

INTRODUCTION

In research and teaching in nuclear engineering a neutron source with a fission spectrum of energies is often desired. It may be used in basic shielding research such as measuring removal cross sections and parameters for determining the production of secondary gamma rays. Specific reactor shield designs of complex geometry with irregularly shaped ducts may be checked experimentally with such a source. It may be used as a source of fast neutrons in studies of radiation effects on reactor components or materials for use in fast neutron fluxes.

In a thermal reactor such as the UTR-10 only thermal neutrons or a mixture of thermal and epithermal neutrons are available in the experimental facilities. One of the simplest methods of obtaining a source of fission spectrum neutrons is to place a plate containing U^{235} across the end of a reactor thermal column such as the graphite duct leading from the core of the UTR-10 to the shield tank. The thermal neutrons diffusing through the duct will produce fissions in the U^{235} in the plate and the resulting fission neutrons will then be emitted into the shield tank where the materials to be tested are placed. A uranium bearing plate of this type is called a "converter plate" or "fission plate" for obvious reasons.

The design of a system like the one described involves many problems. If the device is to contain fissionable material the first and most important step is to determine whether or not it is safe. Calculations must be made to verify that the particular combination of materials used in a particular geometry is subcritical, that is, that

they can not maintain a nuclear chain reaction. If the device is to be used in the vicinity of a nuclear reactor or coupled with a nuclear reactor the combination must be considered. Even if the device itself is subcritical it may produce so large a change in the reactivity of the reactor that the combination of the two would be uncontrollable.

Calculations must also be made to determine the nuclear radiation produced by the device and to determine the shielding required to protect personnel from this radiation. The containment of fission products must be assured.

Because of the serious consequences that may result from an accident or failure in a nuclear facility the calculations must be as accurate as possible. If it is necessary to make assumptions in the development of the theory, care must be used to ensure that the results produced are on the safe side. This procedure will be followed in this project.

REVIEW OF LITERATURE

Information about four fission plate facilities which have been used extensively was found in the literature. Most of the information published about these facilities is concerned with the experimental work conducted at the facility and only a cursory description of the design is given.

The Lid Tank Shielding Facility (LTSF) at Oak Ridge National Laboratory is described in Goldstein (9), Glasstone (6), and Otis (17). This facility was completed in 1949 and consists of a large water tank adjacent to an opening in the seven foot thick concrete shield of the ORNL Standard Graphite Reactor X-10 Pile. The fission plate is placed over this opening between the shield and the water tank. Thermal neutrons escaping from the reactor cause U^{235} in the plate to fission producing the fission spectrum of fast neutrons as well as gamma rays of various energies. The attenuation of these radiations by various combinations of shielding materials placed in the water tank may then be studied.

Two fission plates have been used at the LTSF. The first, designated SP-1, consisted of rows of 1.1 in. O. D. natural uranium slugs stacked one upon the other and held between layers of masonite. The fission reaction was confined to a circle in the center of the plate by placing a boron coated shutter (iris) with a 28-in. diameter circular aperture on the reactor side of the fission plate. A second boron shutter, which could be moved across the opening in the reactor shield so it would absorb the thermal neutrons before they hit the plate, was provided

so that the fission reaction in the plate could be stopped while the reactor was still operating. A third boron shutter was placed on the lid tank side of the fission plate to prevent shielding samples from reflecting thermal neutrons into the fission plate and thus causing fluctuations in the source strength of the plate. The power produced in this fission plate was about 1.7 watts according to Otis (17, p. 28).

The second source plate at the LTSF, designated SP-2, replaced SP-1 in 1955. It consists of a circular disk of uranium 28 in. in diameter and 0.06 in. thick enclosed in an aluminum framework and mounted in an opening in the side of the lid tank wall. The uranium in SP-2 is enriched to 20.8% U^{235}. The boron shutter system is essentially the same as that used with SP-1 except that the boron iris is no longer needed. About 5.22 watts of power are produced in this plate.

The designs of the other three fission plate facilities mentioned in the literature are very similar to that of the Oak Ridge LTSF. The principal differences in the facilities are the dimensions, enrichment, and maximum power levels of the fission plates. The fission plate facility at Brookhaven National Laboratory, described by Goldstein (9), is built into the top shield of the reactor with the fission plate on the inside of the reactor shield directly over the core. In this installation three natural uranium fission plates are available and may be used interchangeably. The largest is 40 in. square and the other two are circles of 12 in. and 2 in. diameter respectively. The power produced in the largest fission plate is 43 watts per Mw of reactor power, or a maximum power of 1290 watts when the reactor is at full power of 30 Mw. The

fission plate at Battelle Memorial Institute is described by Morgan et al. (12). The core of this fission plate is 28 in. in diameter, 0.0199 in. thick, and contains 3741 grams of uranium enriched to 93.14% U^{235}. The power produced in the BMI fission plate is about 24 watts during steady-state reactor operations. The fourth fission plate is in the NAIADE facility at the reactor at Fontenay aux Roses, France, and is described briefly by Bourgeois et al. (1) in a paper describing the research work conducted with the facility. This fission plate is natural uranium 2 cm thick and 1 m^2 surface area and is provided with several circular boral diaphragms for varying the effective surface of the fission plate. When the reactor is at 100 Kw the plate emits 4×10^7 neutrons/(cm^2)(sec).

Information about a fifth fission plate was obtained by private communication.[1] The physical dimensions of this plate were 38 cm by 38 cm by 0.01 cm for the highly enriched uranium. The uranium was sandwiched between 2 S aluminum cladding plates 0.7 cm thick. The plate contained 193 grams of U^{235}. When in use this plate was positioned either in the water just outside the graphite reflector of the Ford Nuclear Reactor or in place of six of the outer graphite reflector elements. When inserted in place of water next to the reflector it produced a positive reactivity effect on the reactor of approximately 0.11% $\frac{\Delta k}{k}$. When it replaced graphite in the reflector a negative reactivity change of approximately 0.34% $\frac{\Delta k}{k}$ resulted. The maximum power developed in the fission plate was approximately 8 Kw.

---

[1] Bullock, J. B., Ann Arbor, Michigan. Ford Nuclear Reactor fission plate. Private communication. 1963.

Except for the reactivity information given for the Ford Nuclear Reactor, no information was given in the literature concerning the effect of these fission plates on the nuclear reactivity of their respective reactor systems. However, in the design of such a system this effect would be one of the first problems that should be investigated. The primary emphasis in this thesis will be directed toward the determination of the nuclear reactivity effect of the proposed fission plate on the UTR-10 reactor system.

THE EFFECTIVE MULTIPLICATION FACTOR OF THE FISSION PLATE

The fission plate described in this report is to be constructed from several fuel plates of the same type as those used in the UTR-10 core. The over-all dimensions of the fuel plates are 26 in. by 3 in. by 0.080 in. These fuel plates contain approximately 92% enriched uranium metal in a uranium-aluminum matrix. The matrix is approximately 0.040 in. thick and is clad with 0.020 in. of aluminum. The total fuel loading per plate is approximately 23 g of U^{235} and the area of the plate containing the fuel is approximately 23 in. by 2.75 in. The fission plate will be made up of two layers of these fuel plates in an overlapping arrangement. For the nuclear physics calculations the narrow strips of pure aluminum at the edges of the fuel plates will be ignored, and it will be assumed that the fission plate has a uniform loading of U^{235}.

This fission plate will be placed in the water-filled shield tank of the UTR-10 reactor against the aluminum thermal duct window as shown in Fig. 1. Thermal neutrons diffusing out through the graphite thermal duct from the UTR-10 core will cause fissioning of U^{235} in the plate thus producing a source of fast neutrons with a fission spectrum. These fission neutrons will pass into the graphite and water media surrounding the plate where they will be thermalized. Eventually some of the neutrons that originated in the fission plate may diffuse back to the plate and cause more fissioning. Thus a multiplication of the thermal flux at the plate may occur.

The multiplication of the thermal flux may be considered in the following manner. Let ϕ_s be the original thermal neutron flux at the

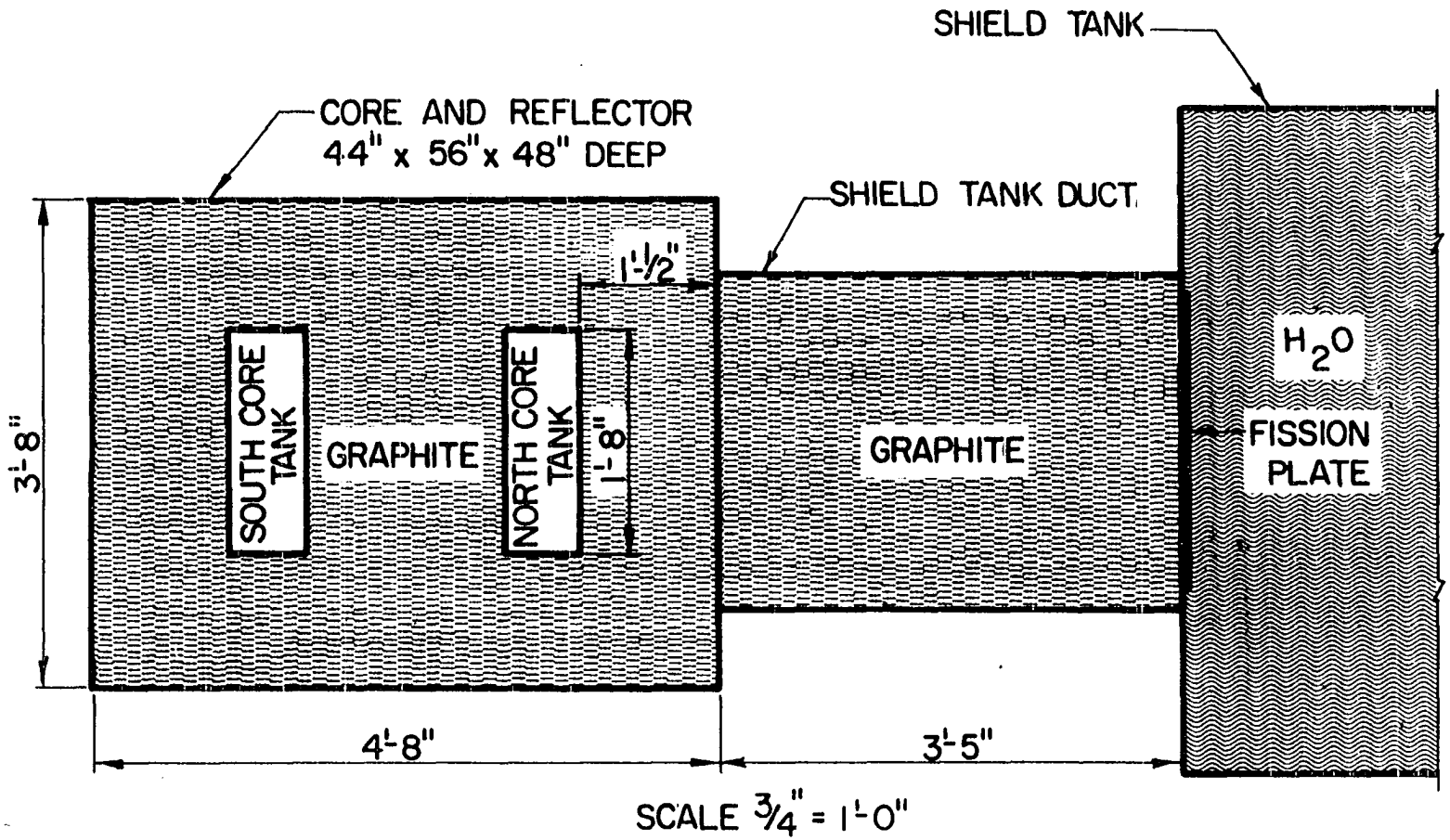

Fig. 1. Top view of UTR-10 core and shield tank duct

plate position without the plate being present. Let $\bar{\phi}_1$, $\bar{\phi}_2$, ... stand for the total thermal flux at the plate after the 1, 2, ... generations of neutrons from the plate, and let ϕ_1, ϕ_2, ... be the thermal flux at the plate due to the 1, 2, ... generations of fission neutrons. Then if C is the multiplication factor of the plate for each generation of neutrons, after one generation

$$\bar{\phi}_1 = \phi_s + C\phi_s = \phi_s + \phi_1 \cdot \tag{1}$$

After 2 generations

$$\bar{\phi}_2 = \phi_s + C\bar{\phi}_1 = \phi_s + C\phi_s + C^2\phi_s \tag{1a}$$

and after n generations

$$\bar{\phi}_n = \phi_s \left(1 + C + C^2 + \ldots + C^n\right) . \tag{1b}$$

The C in the above equation is really the effective multiplication factor for the fission plate-graphite-water system and if it is less than one the series is convergent. Thus if C is less than one the system is subcritical and the neutron flux rapidly approaches an equilibrium value as n approaches infinity and the total equilibrium flux at the plate is given by

$$\bar{\phi} = \phi_s \left(\frac{1}{1 - C}\right) . \tag{2}$$

The total multiplication of the plate is thus given by $\frac{1}{1 - C}$.

The problem now is to determine C for the fission plate and geometry of the proposed UTR-10 installation. As can be seen from Eq. 1,

$$C = \frac{\phi_1}{\phi_s} \quad . \tag{3}$$

Therefore ϕ_1 must be found in terms of ϕ_s. Hwang (11) has developed a

theoretical solution of this problem based on diffusion theory.

Consider the origin of coordinates at the center of the fission plate with the x axis along the center line of the thermal duct. Then the equation for ϕ_1 at x = 0 as given by Hwang (11, p. 15) is

$$\phi_1(0) = \frac{S_1}{1 - \frac{D_g B_g}{D_w B_w} - \frac{t_p \Sigma_{ap}}{D_w B_w}} \left\{ \frac{\Sigma_o}{4 D_w B_w^2} \ln \left(\frac{\Sigma_o + B_w}{B_w - \Sigma_o} \right) - \frac{e^{B_g^2 \tau_g}}{2 D_w B_w} \left[1 - e^{-l^2/4\tau_g} \right] \left[1 - \operatorname{erf} \left(B_g \sqrt{\tau_g} \right) \right] \right\} \qquad (4)$$

where ϕ_1 is assumed to have a cosine distribution in the y and z directions going to zero at the extrapolated dimensions of the thermal duct.

S_1 = the source strength of first generation fission neutrons at the center of the plate and thus is proportional to ϕ_s.

D_g = thermal diffusion coefficient in graphite

D_w = thermal diffusion coefficient in water

$$B_g = \sqrt{\left(\frac{\pi}{a}\right)^2 + \left(\frac{\pi}{b}\right)^2 + \frac{\Sigma_{ag}}{D_g}}$$

$$B_w = \sqrt{\left(\frac{\pi}{a}\right)^2 + \left(\frac{\pi}{b}\right)^2 + \frac{\Sigma_{aw}}{D_w}}$$

a = extrapolated dimension of the thermal duct in the y direction

b = extrapolated dimension of the thermal duct in the z direction

Σ_{ag} = macroscopic thermal absorption cross-section of graphite

Σ_{aw} = macroscopic thermal absorption cross-section of water

t_p = thickness of fission plate

Σ_{ap} = macroscopic thermal absorption cross-section of the fission plate

Σ_o = the fast removal cross-section for water = $\frac{1}{\sqrt{3\,\tau_w}}$

τ_w = age of thermal neutrons in water

τ_g = age of thermal neutrons in graphite

ℓ = equivalent radius of fission plate

Hwang obtained Eq. 4 by solving the following diffusion equations.

$$D_g \nabla^2 \phi_{1g}(x,y,z) - \Sigma_{ag}\phi_{1g}(x,y,z) + \frac{S_1(0,y,z)e^{-x^2/4\tau_g}}{\sqrt{4\pi\tau_g}}\left(1 - e^{-\ell^2/4\tau_g}\right) = 0 \quad (5)$$

$$D_w \nabla^2 \phi_{1w}(x,y,z) - \Sigma_{aw}\phi_{1w}(x,y,z) + \left[-S(0,y,z)\frac{\Sigma_o}{2} E_i(-\Sigma_o x)\right] = 0 \quad (6)$$

The source term in Eq. 5 for the graphite medium was obtained by assuming that the fission plate was a finite plane source of radius ℓ with a uniform strength of one fast neutron per cm^2 per second. The slowing down density kernel for a point source was then integrated over the plane source to obtain the term

$$\frac{e^{-x^2/4\tau_g}}{\sqrt{4\pi\tau_g}}\left(1 - e^{-\ell^2/4\tau_g}\right).$$

However, the source distribution is actually dependent on ϕ_s and would thus have a cosine distribution in the y and z directions. Therefore, the assumption would exaggerate the magnitude of the slowing down density at position x and give a larger $\phi_1(0)$ and in turn a larger multiplication

factor C than the actual value. Since Fermi Age theory does not apply in a water medium, Hwang obtained the source term in Eq. 6 for the water medium by using the single collision slowing down kernel suggested by Weinberg and Wigner (21, p. 402):

$$K_{pt}(\vec{r}, \tau) = \frac{\Sigma_o e^{-\Sigma_o r}}{4\pi r^2} \quad , \tag{7}$$

where r is the distance from the point source to the position where the slowing down density is measured. This kernel was also integrated over the finite plane source of radius ℓ , and, by assuming that ℓ was large, the approximate value for the slowing down density in water was found to be

$$-\frac{\Sigma_o}{2} E_i(-\Sigma_o x).$$

This term exaggerates the slowing down density in water for the same reason as discussed above in the graphite medium case and also because ℓ was assumed to be large. If ℓ is small the slowing down density at position x would be less than that given by this term.

The thermal neutron fluxes $\phi_{1g}(x,y,z)$ and $\phi_{1w}(x,y,z)$ and the fast source term $S_1(0,y,z)$ were then assumed to be separable in the x,y,z directions and to have the form $\cos\frac{\pi y}{a}$ and $\cos\frac{\pi z}{b}$ in the y and z directions. Eqs. 5 and 6 were thus reduced to the following one dimensional form in x:

$$\frac{d^2\phi_{1g}(x)}{dx^2} - B_g^2\phi_{1g}(x) + \frac{S_1 e^{-x^2/4\tau_g}}{D_g\sqrt{4\pi\,\tau_g}}\left(1 - e^{-\ell^2/4\tau_g}\right) = 0 \tag{8}$$

and

$$\frac{d^2\phi_{1w}(x)}{dx^2} - B_w^2\phi_{1w}(x) + \frac{1}{D_w}\left[-S_1\frac{\Sigma_o}{2}E_i(-\Sigma_o x)\right] = 0 \ . \qquad (9)$$

These equations were then solved by Fourier transform techniques. The solution of Eq. 8 is

$$\phi_{1g}(x) = e^{-B_g x}\phi_{1g}(0)$$

$$+ \frac{S_1 e^{B_g^2\tau_g}}{4D_g B_g}\left(1 - e^{-x^2/4\tau_g}\right)\left\{e^{B_g x}\left[1 - \operatorname{erf}\left(\frac{x}{2\sqrt{\tau_g}} + B_g\sqrt{\tau_g}\right)\right]\right.$$

$$\left. - e^{-B_g x}\left[1 - \operatorname{erf}\left(\frac{x}{2\sqrt{\tau_g}} - B_g\sqrt{\tau_g}\right) - 2\operatorname{erf}\left(B_g\sqrt{\tau_g}\right)\right]\right\} , \qquad (10)$$

and the solution of Eq. 9 is

$$\phi_{1w}(x) = \frac{S_1}{2D_w}\frac{\Sigma_o}{B_w^2}\left\{E_1(\Sigma_o x) - \frac{e^{B_w x}}{2}E_1\left[\Sigma_o x\left(1 + \frac{B_w}{\Sigma_o}\right)\right] - \frac{e^{-B_w x}}{2}E_1\left[\Sigma_o x\left(1 - \frac{B_w}{\Sigma_o}\right)\right]\right.$$

$$\left. + \frac{e^{-B_w x}}{2}\ln\left(\frac{\Sigma_o + B_w}{B_w - \Sigma_o}\right)\right\} - \phi'_{1w}(0)\frac{e^{-B_w x}}{B_w} \ , \qquad (11)$$

where $\phi'_{1w}(0)$ is the first derivative with respect to x of $\phi_{1w}(x)$ evaluated at x = 0.

In order to determine the constants $\phi_{1g}(0)$ and $\phi'_{1w}(0)$, Hwang assumed the following boundary conditions suggested by Galanin (4) for a thin slab of neutron absorbing material placed at the interface between two different media:

1. The neutron flux at the fission plate is continuous,

$$\phi_{1g}(0) = \phi_{1w}(0) \ . \qquad (12)$$

2. The net thermal neutron currents at either side of the plate are not equal due to the fact that there will be neutron absorption in the plate. However, the difference between these two quantities is equal to the number of neutrons absorbed per unit time per unit area in the fission plate. That is

$$-D_w \phi'_{1w}(0) + D_g \phi'_{1g}(0) = t_p \Sigma_{ap} \phi_{1w}(0) \quad . \tag{13}$$

Eqs. 10 and 11 along with these boundary conditions were then solved as simultaneous equations at x = 0 for $\phi_{1g}(0)$ as given in Eq. 4.

The values of the parameters entering into Eq. 4 are listed in Table 1. The nuclear parameters were all obtained from Nowak and Chow (15, p. 26). The neutron cross-sections given in the table have been corrected

Table 1. Parameters for Eq. 4

$D_g = 0.903$ cm	$\Sigma_{ap} t_p = 0.1740$
$D_w = 0.160$ cm	$S_1 = 0.3592\ \phi_s(0) \frac{\text{fast neutrons}}{\text{cm}^2\ \text{sec}}$
$\tau_g = 350\ \text{cm}^2$	$\ell = 30.48$ cm
$\Sigma_{ag} = 0.00036\ \text{cm}^{-1}$	a = b = 100 cm
$\Sigma_{aw} = 0.0197\ \text{cm}^{-1}$	
$\tau_w = 33\ \text{cm}^2$	

for a Maxwell-Boltzmann distribution and also by the not 1/v factor where applicable. The value of ℓ was obtained from the dimensions of the fuel bearing area of the UTR-10 fuel plates.

The value given for a and b is a somewhat arbitrary exaggeration of the extrapolated dimensions of the graphite thermal duct in the y and z directions to provide a safety factor in the calculations. The actual dimensions of the graphite duct are 30 in. by 30 in. or 76.2 cm by 76.2 cm and the extrapolated dimensions for a black boundary would be 80.1 cm by 80.1 cm. However, the duct is surrounded by concrete which is not a completely black boundary for thermal neutrons. A few neutrons will be scattered back into the duct from the concrete and thus produce a small reflector savings. For a situation of this type Nowak (14, p. 2) states that "it is known experimentally that the albedo of most shield materials through which the duct will extend is low, so this flux gain from such reflection will be small." Hwang has also tried to measure these extrapolated dimensions of the UTR-10 thermal duct by mapping the thermal flux with indium foils placed against the water side of the thermal duct window. He fitted a cosine curve to his data by means of a least squares procedure and then extrapolated the curve to zero to obtain the dimensions a = 101.6 cm and b = 96.5 cm. These values would substantiate the value of 100 cm used in this calculation but it should be remembered that they were measured in the water of the shield tank and not actually in the graphite duct.

The quantities S_1 and $\Sigma_{ap} t_p$ were obtained by assuming that the plate was made up of U^{235} only. Ignoring the small amount of U^{238} and the aluminum does not affect the results significantly since their cross-sections are very small compared to U^{235}. Also their effect would be mainly the absorption of thermal neutrons and thus a depression of the flux in the

U^{235} and, therefore, of the multiplication in the plate. If N_p^{25} is the number of U^{235} nuclei per cm^2 of a fission plate made up of two layers of UTR-10 fuel plates, then, assuming 23 g of U^{235} per fuel plate and the dimensions given, it is found that

$$N_p^{25} = 2.886 \times 10^{20} \frac{U^{235} \text{ nuclei}}{cm^2} . \tag{14}$$

Then

$$\Sigma_{ap} t_p = N_p^{25} \sigma_a^{25} = 0.1740 \tag{15}$$

and if $\nu = 2.46$ is the number of fast neutrons produced per fission in U^{235} as given by Hughes and Schwartz (10)

$$S_1 = N_p^{25} \sigma_f^{25} \nu \phi_s(0) = 0.3592 \phi_s(0) \frac{\text{fast neutrons}}{cm^2 \text{ sec}} . \tag{16}$$

When these parameters are inserted in Eq. 4, $\phi_{1g}(0)$ is found to be

$$\phi_{1g}(0) = 0.1522 \phi_s(0) , \tag{17}$$

and therefore

$$C = \frac{\phi_{1g}(0)}{\phi_s(0)} = 0.1522 . \tag{18}$$

The total multiplication of the plate would thus be

$$\frac{1}{1 - C} = 1.180 . \tag{19}$$

The value of C found above is a low value for an effective multiplication factor of a system and means that the fission plate-graphite-water system is subcritical. However, this value should be considered only a first order approximation for the actual multiplication factor for two reasons. The boundary conditions used by Hwang are strictly applicable

only for a very thin slab of not too strongly absorbing material at the boundary between the two mediums and, also, these equations are based on diffusion theory which is not accurate near boundaries and sources. As applied above to find C, both of these limitations are violated.

In order to allow for these uncertainties the value of C to be used in the remaining calculations will be assumed to be 0.50. When this value of C is used the total multiplication of the thermal flux by the fission plate is found to be 2. This is a reasonable value to choose when compared to experimental results obtained with the Battelle Memorial Institute fission plate. According to Morgan et al. (12), the BMI fission plate consists of a foil of 93.14% enriched uranium 28 in. in diameter clad with aluminum. It contains a total of 3484 g of U^{235} which is about 9 times as much as will be in the UTR-10 fission plate. The fission plate at Battelle is normally used with a 1/4-in. boral plate attached to the water side so that effectively all of the thermal neutrons returning from the water are stopped before they reach the U^{235}. However, it has been observed that the power of the fission plate is increased by a factor of 1.36 when the boral plate is removed. Such an increase in power would be directly proportional to the increase in thermal flux in the plate and thus to the total multiplication of the plate as defined. The multiplication due to return of neutrons from the graphite side would be less because of the relatively small size of the graphite duct, and the fact that the neutrons travel much farther in graphite than in water before being thermalized. Thus, the total multiplication factor for the BMI fission plate would be less than 2. Since the proposed UTR-10 fission

plate is smaller in area and has less fuel than the BMI fission plate its total multiplication factor should be less than that for the BMI plate.

THE EFFECT ON THE REACTIVITY OF THE REACTOR

Now that it has been determined that the fission plate itself in its graphite-water medium is subcritical the next step is to determine if the presence of the fission plate causes any significant change in the reactivity of the reactor. The reactivity effect of the fission plate will be investigated by three different methods. These are 1) perturbation theory, 2) two-group diffusion theory, and 3) an analogy between the increased neutron flux at the core boundary and a hypothetical increase in the nonleakage probability to give the same effect.

Perturbation Theory

The perturbation theory approach is based on the theory presented by Webster (20). A fictitious change in the infinite medium multiplication factor k_∞, represented by $\overline{\Delta k}$, is found that would have the same effect on the reactor period (or on the effective multiplication factor k_{eff}) as all the actual changes, i. e. including changes in P_1 and P_2 (fast and thermal nonleakage factors). Then Webster used the following relation for the change in reactivity

$$\Delta \rho = \frac{\Delta k_{eff}}{k_{eff}} = \frac{\overline{\Delta k}}{\overline{k_f}} \quad , \tag{20}$$

where $\overline{k_f} = k_\infty + \overline{\Delta k}$.

Webster (20, p.11) gives the following relation for $\overline{\Delta k}$ for uniform changes in the reflector of a cylindrical reactor:

$$\overline{\Delta k} = \frac{1}{\int_0^{r_c} \Sigma_a \phi_1^* \phi_2 r dr} \left[\delta D_1 \int_{r_c}^{\infty} \phi_1^* \frac{\phi_1}{\tau} r dr + \delta D_1 \phi_1^*(r_c) \left(\frac{\partial \phi_1}{\partial r} \right)_{r_c} r_c \right.$$

$$+ \delta \left(\frac{D_1}{\tau} \right) \int_{r_c}^{\infty} \phi_1 (\phi_2^* - \phi_1^*) r dr + \delta D_2 \int_{r_c}^{\infty} \phi_2^* \left(\frac{\Sigma_a}{D_2} \phi_2 - \frac{D_1}{D_2 \tau} \phi_1 \right) r dr$$

$$\left. + \delta D_2 \phi_2^*(r_c) \left(\frac{\partial \phi_2}{\partial r} \right)_{r_c} r_c - \delta \Sigma_a \int_{r_c}^{\infty} \phi_2^* \phi_2 r dr \right] , \qquad (21)$$

where the subscripts 1 and 2 refer to fast and thermal neutrons respectively, r_c is the radius of the core, Σ_a, D, and τ have their usual meaning, and ϕ_1^* and ϕ_2^* are the fast and thermal adjoint-flux distributions respectively (sometimes called the fast and thermal importance functions).

For an infinite slab reactor Eq. 21 becomes

$$\overline{\Delta k} = \frac{1}{\int_{\text{Core}} \Sigma_a \phi_1^* \phi_2 dx} \left[\delta D_1 \int_{x_c}^{\infty} \phi_1^* \frac{\phi_1}{\tau} dx + \delta D_1 \phi_1^*(x_c) \left(\frac{\partial \phi_1}{\partial x} \right)_{x_c} \right.$$

$$+ \delta \left(\frac{D_1}{\tau} \right) \int_{x_c}^{\infty} \phi_1 (\phi_2^* - \phi_1^*) dx + \delta D_2 \int_{x_c}^{\infty} \phi_2^* \left(\frac{\Sigma_a}{D_2} \phi_2 - \frac{D_1}{D_2 \tau} \phi_1 \right) dx$$

$$\left. + \delta D_2 \phi_2^*(x_c) \left(\frac{\partial \phi_2}{\partial x} \right)_{x_c} - \delta \Sigma_a \int_{x_c}^{\infty} \phi_2^* \phi_2 dx \right] . \qquad (22)$$

This equation may be used for the finite UTR-10 reactor if the neutron leakage in the y and z directions is taken into account. In the fifth term in the brackets of Eq. 22 the quantity $\delta D_2 \left(\frac{\partial \phi_2}{\partial x} \right)_{x_c}$ expresses the change in the rate of appearance (leakage) of thermal neutrons at the

surface of the core. Leakage into the core produces positive $\overline{\Delta k}$. Multiplication by $\phi_2^*(x_c)$ establishes the importance of these extra neutrons at the core-reflector interface. The second term in the brackets accomplishes the same thing for the fast neutron leakage.

If a fission plate is added at the end of the graphite duct it acts as a source of neutrons and produces a current of fast and thermal neutrons into the core. Thus, the effect of the fission plate on the reactivity of the reactor is given by the second and fifth terms in the brackets of Eq. 22. The rest of the terms are zero because no changes have been made in the physical parameters of the reactor. So, if the current of fast and thermal neutrons into the core produced by the fission plate and the importance functions $\phi_1^*(x_c)$ and $\phi_2^*(x_c)$ for these neutrons can be found, Eq. 22 may be used to find $\overline{\Delta k}$ and thus $\Delta\rho$ produced by the fission plate.

Hwang (11) gives an equation for the total thermal flux at position x in the graphite duct due to the fission plate. In this equation x is measured from the fission plate. If the assumed multiplication factor of 2 is used, this equation is

$$\phi_g(x) = \phi_s(0)e^{-B_g x} + \frac{Se^{B_g^2 \tau_g}}{4D_g B_g}\left(1 - e^{-\ell^2/4\tau_g}\right)\left\{e^{B_g x}\left[1 - \operatorname{erf}\left(\frac{x}{2\sqrt{\tau_g}} + B_g\sqrt{\tau_g}\right)\right] - e^{-B_g x}\left[1 - \operatorname{erf}\left(\frac{x}{2\sqrt{\tau_g}} - B_g\sqrt{\tau_g}\right) - 2\operatorname{erf}\left(B_g\sqrt{\tau_g}\right)\right]\right\} \qquad (23)$$

where $S = 2N_p^{25}\sigma_f^{25}\nu\phi_s(0)$. This equation, based on diffusion theory,

should be accurate at distances greater than two mean free paths from the fission plate.

The derivative of Eq. 23 with respect to x is

$$\frac{\partial \bar{\phi}_g(x)}{\partial x} = -B_g \phi_s(0) e^{-B_g x}$$

$$+ \frac{Se^{B_g^2 \tau_g}}{4D_g B_g} \left(1 - e^{-\ell^2/4\tau_g}\right) \left\{ B_g e^{B_g x} \left[1 - \operatorname{erf}\left(\frac{x}{2\sqrt{\tau_g}} + B_g\sqrt{\tau_g}\right)\right] \right.$$

$$- \frac{1}{\sqrt{\pi\,\tau_g}} e^{B_g x} e^{-\left(x/2\sqrt{\tau_g} + B_g\sqrt{\tau_g}\right)^2}$$

$$+ B_g e^{-B_g x} \left[1 - \operatorname{erf}\left(\frac{x}{2\sqrt{\tau_g}} - B_g\sqrt{\tau_g}\right) - 2\operatorname{erf}\left(B_g\sqrt{\tau_g}\right)\right]$$

$$\left. + \frac{1}{\sqrt{\pi\tau_g}} e^{-B_g x} e^{-\left(x/2\sqrt{\tau_g} - B_g\sqrt{\tau_g}\right)^2} \right\}. \qquad (24)$$

If Eq. 24 is evaluated at x = 137 cm and the result multiplied by the diffusion coefficient in graphite the current of thermal neutrons at the surface of the core of the reactor is obtained. Thus

$$D_g \frac{\partial \bar{\phi}_g(137)}{\partial x} = -46.17 \times 10^{-5} \phi_s(0) \ . \qquad (25)$$

Since the origin of coordinates for this calculation was taken at the fission plate and x increases toward the reactor, the minus sign indicates a flow of neutrons into the reactor owing to the fission plate. Therefore

$$\delta D_2 \left(\frac{\partial \phi_2}{\partial x}\right)_{x_c} = -D_g \frac{\partial \bar{\phi}_g(137)}{\partial x} = 46.17 \times 10^{-5} \phi_s(0) \ . \qquad (26)$$

The fast neutron flux, produced by the fission plate, at position x on the center line of the graphite duct is

$$\phi_1(x) = \frac{S}{2\bar{\mu}_1 D_1} e^{-\bar{\mu}_1 x} \tag{27}$$

where

$$S = 2N_p^{25}\sigma_f^{25}\nu\phi_s(0)$$

$$\bar{\mu}_1^2 = \frac{1}{\tau_g} + \left(\frac{\pi}{a}\right)^2 + \left(\frac{\pi}{b}\right)^2$$

D_1 = the diffusion coefficient for fast neutrons.

The current of fast neutrons in the graphite duct at distance x from the fission plate is thus

$$-D_1\frac{\partial\phi_1(x)}{\partial x} = \frac{S}{2} e^{-\bar{\mu}_1 x} . \tag{28}$$

When Eq. 28 is evaluated at x = 137 cm the current of fast neutrons into the core of the reactor from the fission plate is found to be

$$\delta D_1\left(\frac{\partial\phi_1}{\partial x}\right)_{x_c} = -D_1\frac{\partial\phi_1(137)}{\partial x} = 2.62 \times 10^{-5}\,\phi_s(0) . \tag{29}$$

The problem now is to find $\phi_s(0)$ and a corresponding value for $\phi_1^*(x_c)$ and $\phi_2^*(x_c)$. Nowak and Chow (15, Fig. 38) give curves of relative values of ϕ_1, ϕ_1^*, and ϕ_2 and ϕ_2^* vs distance from the center line in the UTR-10 core. From these curves the relative values of ϕ_1^*, ϕ_2^* and ϕ_2 at the outer surface of the core tank are $\phi_1^* = 6.91$, $\phi_2^* = 8.90$ and $\phi_2 = 6.79$. So if $\phi_s(0)$ (the thermal flux at the fission plate position without the

fission plate present) is found in terms of ϕ_2 at the surface of the core tank, these relative values of ϕ_1^*, ϕ_2^* and ϕ_2 may be used with Eq. 26 and Eq. 29 to find $\int D_1 \phi_1^*(x_c)\left(\frac{\partial \phi_1}{\partial x}\right)_{x_c}$ and $\int D_2 \phi_2^*(x_c)\left(\frac{\partial \phi_2}{\partial x}\right)_{x_c}$.

Nowak (14) gives an equation based on two group diffusion theory for the transmission of neutron flux through rectangular graphite ducts. The thermal flux in an infinitely long duct at a distance x from a unit source of fast flux at the end of the duct is

$$\phi_2(x) = \beta\left(e^{-\bar{H}_2 x} - e^{-\bar{H}_1 x}\right) \tag{30}$$

where

$$\beta = \frac{H_2^2\, \rho}{H_1^2 - H_2^2}$$

$$H_1^2 = \frac{1}{\tau_g}$$

$$H_2^2 = \frac{\Sigma_{ag}}{D_g}$$

$$\rho = \frac{\Sigma_1}{\Sigma_{ag}}$$

Σ_1 = the slowing down cross-section in graphite for the fast group

$$\bar{H}_1^2 = H_1^2 + \left(\frac{\pi}{a}\right)^2 + \left(\frac{\pi}{b}\right)^2$$

$$\bar{H}_2^2 = H_2^2 + \left(\frac{\pi}{a}\right)^2 + \left(\frac{\pi}{b}\right)^2 = B_g^2 \text{ defined above.}$$

The subscripts 1 and 2 stand for fast and thermal groups respectively. The thermal flux at distance x from a unit source of thermal flux at the end of the duct is simply

$$\phi_2(x) = e^{-\overline{\mu}_2 x} \quad . \tag{31}$$

In both cases the origin of coordinates is taken at the center of the source end of the duct and the flux distribution in the y and z directions is given by $\cos \frac{\pi y}{a}$ and $\cos \frac{\pi z}{b}$ respectively.

Nowak and Chow (15, p. 7) state that the ratio, m, of thermal to fast flux at the interface between the core tank and the graphite reflector in the UTR-10 is 0.3. Therefore, the magnitude of the fast neutron flux at this interface is 3.33 times that of the thermal flux. If this fact is used, Eqs. 30 and 31 may be combined to obtain the following equation for the total thermal neutron flux, $\phi_2(x)$, at position x in the graphite duct (measured from the core tank) when the thermal flux at the surface of the core tank is unity.

$$\phi_2(x) = 3.33\beta\left(e^{-\overline{\mu}_2 x} - e^{-\overline{\mu}_1 x}\right) + e^{-\overline{\mu}_2 x} \tag{32}$$

The values of all the parameters entering into this equation have been given except Σ_1. Nowak and Chow (15, p. 26) give 0.00314 cm^{-1} for the value of Σ_1.

In the UTR-10 the length of the graphite duct is 54 in. or 137 cm. Therefore, for a unit thermal flux at the surface of the core tank, $\phi_2(137)$ equals $\phi_s(0)$ as defined. When the parameters given are used $\phi_s(0)$ is found to be 6.885×10^{-3} thermal neutrons per cm^2 per sec per unit

thermal flux at the surface of the core tank. If this value is substituted for $\phi_s(0)$ in Eq. 26 and if the relative values of ϕ_2^* and ϕ_2 at the surface of the core tank are used, it is found that the relative value of the importance weighted current of thermal neutrons into the core due to the fission plate is

$$\delta D_2 \phi_2^*(x_c) \left(\frac{\partial \phi_2}{\partial x}\right)_{x_c} = 1.921 \times 10^{-4} \quad . \tag{33}$$

The relative value of the importance weighted current of fast neutrons flowing into the core from the fission plate is similarly found from Eq. 29 to be

$$\delta D_1 \phi_1^*(x_c) \left(\frac{\partial \phi_1}{\partial x}\right)_{x_c} = 0.084 \times 10^{-4} \quad . \tag{33a}$$

The relative value for $\int_{\text{core}} \Sigma_a \phi_1^* \phi_2 dx$ is found to be 73.77 by calculating an average value of Σ_a for the theoretically homogenized core and using the relative values of $\int_{\text{core}} \phi_1^* \phi_2 dx$ for the UTR-10 core given by Nowak and Chow (15, p. 24). If these values are substituted in Eq. 22, $\overline{\Delta k}$ is found to be

$$\overline{\Delta k} = \frac{(1.921 + 0.084)10^{-4}}{73.77} = 2.718 \times 10^{-6} \quad . \tag{34}$$

Now, if Eq. 34 is substituted into Eq. 20, the latter becomes

$$\Delta \rho = \frac{2.718 \times 10^{-6}}{k_\infty + 2.718 \times 10^{-6}} \quad . \tag{35}$$

$\overline{\Delta k}$ in the denominator of Eq. 35 is negligible compared to k_∞ so

$$\Delta\rho \simeq \frac{2.718 \times 10^{-6}}{k_\infty} \quad . \tag{36}$$

Since ϵ and p are approximately unity for the highly enriched UTR-10 an approximate value for k_∞ may be found from

$$k_\infty \simeq \eta f = \frac{\nu \bar{\Sigma}_f}{\bar{\Sigma}_a^U} \frac{\bar{\Sigma}_a^U}{\bar{\Sigma}_a} = \frac{\nu \bar{\Sigma}_f}{\bar{\Sigma}_a} \tag{37}$$

where the bars over the terms indicate average values for the homogenized core. From Eq. 37, k_∞ is found to be approximately 1.640 and so

$$\Delta\rho \simeq \frac{2.718 \times 10^{-6}}{1.640} = 1.657 \times 10^{-6} \frac{\Delta k}{k} \quad . \tag{38}$$

This result indicates that the fission plate has a small effect on the reactivity of the reactor and that the addition of the fission plate to the system will produce no nuclear control problems. However, this value for $\Delta\rho$ will be checked by two other methods of calculation in the succeeding sections of this work.

Two-Group Diffusion Theory

Two-group diffusion theory is discussed at length in such references as Murray (13), Glasstone and Edlund (7), and Weinberg and Wigner (21). In this theory the neutrons in the reactor are classified into two groups according to neutron energy. One is the usual thermal group and the second is the so-called fast group which is a mathematical composite of all neutrons other than thermals. The subscript 1 is used to designate the parameters associated with the fast group and subscript 2 for those associated with the thermal group. Diffusion equations are written for each

group, and then these equations are solved as simultaneous differential equations dependent on certain boundary conditions.

The procedure used in this calculation will be the matrix method described by Garabedian and Householder (5) for solving the critical equation of a multi-region reactor. It consists of reducing the critical determinant for any number of regions to a determinant of the same form as that of the two-region problem. This is done by a series of matrix multiplications and inversions. The problem is first solved for the critical fuel loading of the basic reactor without the fission plate. Then this fuel loading is used, and the problem solved again for the fictitious change in ν necessary to make the reactor just critical with the fission plate in place. The change in reactivity produced by the fission plate is then found from the standard equation presented in references such as Webster (20) and Weinberg and Wigner (21):

$$\Delta\rho = -\frac{\Delta\nu}{\nu} \quad . \tag{39}$$

For the development of the equations the UTR-10 may be considered an infinite slab multi-region reactor. The leakage in the y and z directions is then taken into account by adding the buckling in those directions to $\mathcal{H}_1^2$ and $\mathcal{H}_2^2$ to obtain the square of the effective reciprocal relaxation lengths ($\overline{\mathcal{H}}_1^2$ and $\overline{\mathcal{H}}_2^2$) to use in the working equations. The infinite slab UTR-10 may be represented by the schematic in Fig. 2. Region I is the internal graphite reflector, region II is the north core tank, region III is the graphite reflector and graphite duct leading to the shield tank, and region IV is the shield tank.

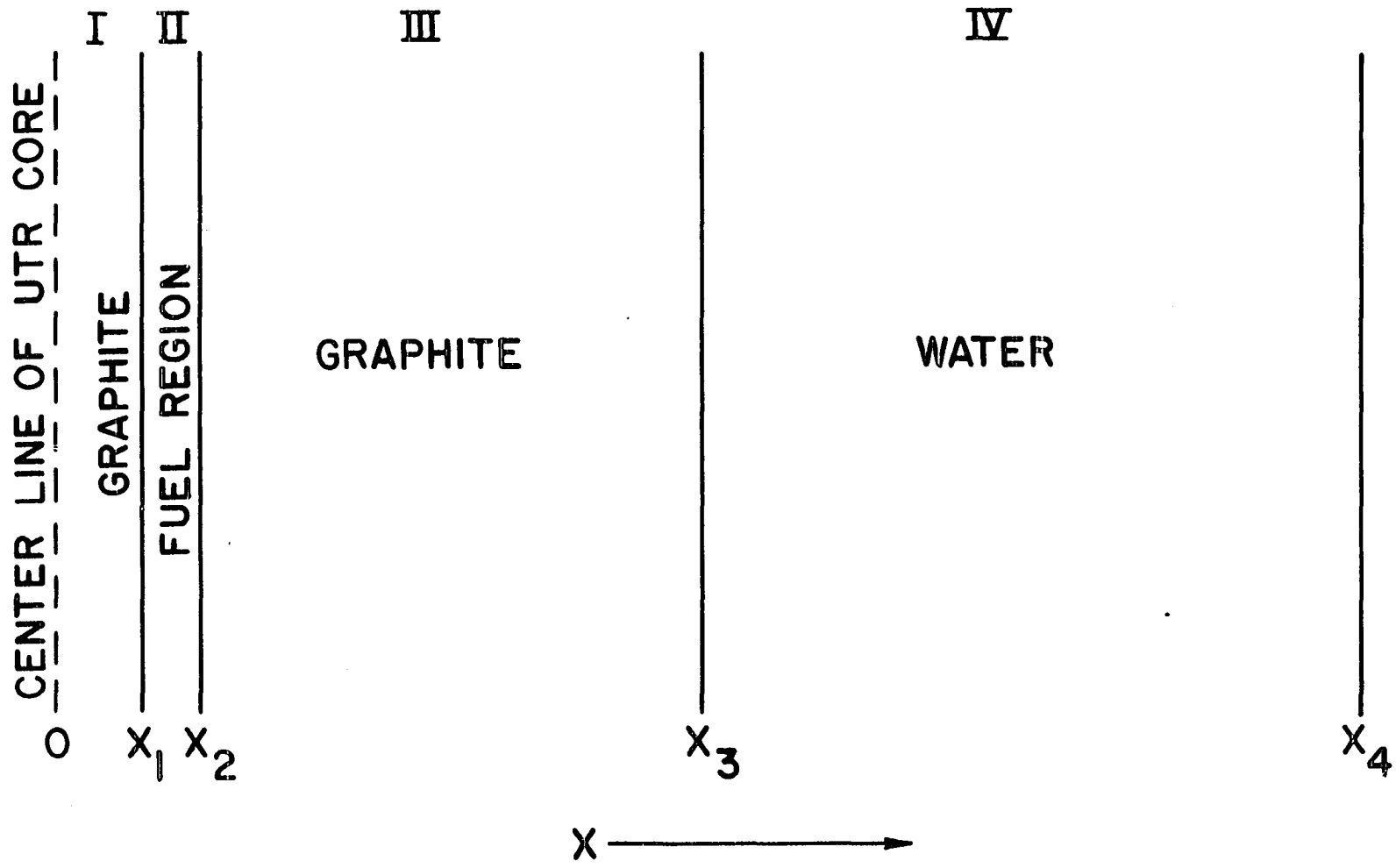

Fig. 2. Schematic of the theoretical infinite slab UTR-10

In region I the diffusion equations are

$$D_{1I}\nabla^2\phi_{1I} - \Sigma_{1I}\phi_{1I} = 0$$
$$D_{2I}\nabla^2\phi_{2I} - \Sigma_{2I}\phi_{2I} + \Sigma_{1I}\phi_{1I} = 0 \tag{40}$$

where the symbols have their usual meaning. The Roman numeral subscripts refer to the region where the symbol applies. Since the UTR-10 core is approximately symmetrical about the plane midway between the two core tanks, it will be assumed that the fast and thermal neutron currents in the x direction vanish at this plane of symmetry. Therefore the solutions of Eqs. 40 are

$$\begin{aligned}
\phi_{1I} &= A_1 \cosh \mathcal{H}_{1I} x \\
\phi_{2I} &= S_I A_1 \cosh \mathcal{H}_{1I} x + A_2 \cosh \mathcal{H}_{2I} x \\
J_{1I} &= D_{1I} \mathcal{H}_{1I} A_1 \sinh \mathcal{H}_{1I} x \\
J_{2I} &= D_{2I} \mathcal{H}_{1I} S_I A_1 \sinh \mathcal{H}_{1I} x + D_{2I} \mathcal{H}_{2I} A_2 \sinh \mathcal{H}_{2I} x
\end{aligned} \tag{41}$$

where the J's are the negatives of the usual neutron currents, the A_i's are arbitrary coefficients, and

$$\begin{aligned}
\mathcal{H}_{1I}^2 &= \frac{\Sigma_{1I}}{D_{1I}} = \frac{1}{\tau_I} \\
\mathcal{H}_{2I}^2 &= \frac{\Sigma_{2I}}{D_{2I}} = \frac{1}{L_I^2} \\
S_I &= \frac{D_{1I}}{D_{2I}\left(\frac{\tau_I}{L_I^2} - 1\right)} \quad .
\end{aligned} \tag{42}$$

In matrix notation Eqs. 41 may be represented as

$$\underline{\phi}_I(x) = M_I(x)\ a_I \tag{43}$$

where $\underline{\phi}_I(x)$, which will be called the general flux vector, is

$$\underline{\phi}_I(x) = \begin{bmatrix} \phi_{1I} \\ \phi_{2I} \\ J_{1I} \\ J_{2I} \end{bmatrix} \tag{44}$$

and

$$M_I(x) = \begin{bmatrix} \cosh \mathcal{H}_{1I}x & 0 \\ S_I \cosh \mathcal{H}_{1I}x & \cosh \mathcal{H}_{2I}x \\ D_{1I}\mathcal{H}_{1I} \sinh \mathcal{H}_{1I}x & 0 \\ D_{2I}\mathcal{H}_{1I}S_I \sinh \mathcal{H}_{1I}x & D_{2I}\mathcal{H}_{2I} \sinh \mathcal{H}_{2I}x \end{bmatrix} \tag{45}$$

$$a_I = \begin{bmatrix} A_1 \\ A_2 \end{bmatrix} . \tag{46}$$

In region II, the core of the reactor, the diffusion equations are

$$\begin{aligned} D_{1II}\nabla^2\phi_{1II} - \frac{D_{1II}}{\tau_{II}}\phi_{1II} + \Sigma_{2II}f\eta\phi_{2II} &= 0 \\ D_{2II}\nabla^2\phi_{2II} - \Sigma_{2II}\phi_{2II} + \frac{pD_{1II}}{\tau_{II}}\phi_{1II} &= 0 \ . \end{aligned} \tag{47}$$

These equations may be solved by assuming that the fluxes obey the wave equations,

$$\nabla^2\phi_{1II} + B^2\phi_{1II} = 0$$
$$\nabla^2\phi_{2II} + B^2\phi_{2II} = 0 \tag{48}$$

where B^2 is a constant assumed common to both fluxes. When Eqs. 48 are substituted in Eqs. 47 the latter become

$$(1 + B^2\tau_{II})\phi_{1II} - \frac{\Sigma_{2II}\tau_{II}f\eta\phi_{2II}}{D_{1II}} = 0$$
$$-\frac{pD_{1II}\phi_{1II}}{\Sigma_{2II}\tau_{II}} + (1 + B^2L_{II}^2)\phi_{2II} = 0 \quad . \tag{49}$$

If these simultaneous equations are to have other than trivial solutions for ϕ_{1II} and ϕ_{2II}, the determinant formed by the materials-dependent coefficients must be zero. This implies that

$$(1 + B^2\tau_{II})(1 + B^2L_{II}^2) = pf\eta = k_\infty \quad . \tag{50}$$

This quadratic equation in B^2 has two roots, $B^2 = \ell^2$ and $B^2 = -m^2$, where ℓ^2 and m^2 are numerical constants analogous to the materials buckling of age-diffusion theory. In the case of the one-dimensional slab reactor the solutions are

$$\phi_{1II} = B_1\sin \ell x + B_2\cos \ell x + B_3\sinh mx + B_4\cosh mx$$
$$\phi_{2II} = S_{1II}B_1\sin \ell x + S_{1II}B_2\cos \ell x + S_{2II}B_3\sinh mx + S_{2II}B_4\cosh mx$$
$$J_{1II} = D_{1II}\ell B_1\cos \ell x - D_{1II}\ell B_2\sin \ell x + D_{1II}mB_3\cosh mx + D_{1II}mB_4\sinh mx \tag{51}$$
$$J_{2II} = S_{1II}D_{2II}\ell B_1\cos \ell x - S_{1II}D_{2II}\ell B_2\sin \ell x + S_{2II}D_{2II}mB_3\cosh mx$$
$$+ S_{2II}D_{2II}mB_4\sinh mx$$

where ℓ^2 is the material buckling and equals the positive root of Eq. 50, and

$$m^2 = \ell^2 + \frac{1}{L_{II}^2} + \frac{1}{\tau_{II}}$$

$$S_{1II} = \frac{D_{1II}}{\tau_{II} D_{2II}} \left(\frac{1}{\ell^2 + \frac{1}{L_{II}^2}} \right) \tag{52}$$

$$S_{2II} = - \frac{D_{1II}}{\tau_{II} D_{2II}} \left(\frac{1}{\ell^2 + \frac{1}{\tau_{II}}} \right)$$

In matrix notation Eqs. 51 become

$$\vec{\phi}_{II}(x) = M_{II}(x)\ a_{II} \tag{53}$$

where the form of $M_{II}(x)$ is given in Eq. 54 in Table 2, and

$$a_{II} = \begin{bmatrix} B_1 \\ B_2 \\ B_3 \\ B_4 \end{bmatrix} . \tag{55}$$

In region III the diffusion equations are

$$\begin{aligned} D_{1III} \nabla^2 \phi_{1III} - \Sigma_{1III} \phi_{1III} &= 0 \\ D_{2III} \nabla^2 \phi_{2III} - \Sigma_{2III} \phi_{2III} + \Sigma_{1III} \phi_{1III} &= 0 \ . \end{aligned} \tag{56}$$

The solutions of these equations are

$$\begin{aligned} \phi_{1III} &= C_1 \cosh \mu_{1III} x + C_2 \sinh \mu_{1III} x \\ \phi_{2III} &= S_{III} C_1 \cosh \mu_{1III} x + S_{III} C_2 \sinh \mu_{1III} x + C_3 \cosh \mu_{2III} x \\ &\quad + C_4 \sinh \mu_{2III} x \end{aligned} \tag{57}$$

Table 2. Equation 54

$$M_{II}(x) = \begin{bmatrix} \sin \ell x & \cos \ell x & \sinh mx & \cosh mx \\ S_{1II}\sin \ell x & S_{1II}\cos \ell x & S_{2II}\sinh mx & S_{2II}\cosh mx \\ D_{1II}\ell\cos \ell x & -D_{1II}\ell\sin \ell x & D_{1II}m \cosh mx & D_{1II}m \sinh mx \\ S_{1II}D_{2II}\ell\cos \ell x & -S_{1II}D_{2II}\ell\sin \ell x & S_{2II}D_{2II}m \cosh mx & S_{2II}D_{2II}m \sinh mx \end{bmatrix}$$

$$J_{1III} = D_{1III}\mathcal{H}_{1III}C_1 \sinh \mathcal{H}_{1III}x + D_{1III}\mathcal{H}_{1III}C_2 \cosh \mathcal{H}_{1III}x$$

$$J_{2III} = S_{III}D_{2III}\mathcal{H}_{1III}C_1 \sinh \mathcal{H}_{1III}x + S_{III}D_{2III}\mathcal{H}_{1III}C_2 \cosh \mathcal{H}_{1III}x$$
$$+ D_{2III}\mathcal{H}_{2III}C_3 \sinh \mathcal{H}_{2III}x + D_{2III}\mathcal{H}_{2III}C_4 \cosh \mathcal{H}_{2III}x$$

where

$$\mathcal{H}^2_{1III} = \frac{\Sigma_{1III}}{D_{1III}} = \frac{1}{\tau_{III}}$$

$$\mathcal{H}^2_{2III} = \frac{\Sigma_{2III}}{D_{2III}} = \frac{1}{L^2_{III}} \tag{58}$$

$$S_{III} = \frac{D_{1III}}{D_{2III}\left(\frac{\tau_{III}}{L^2_{III}} - 1\right)} \quad .$$

In matrix notation Eqs. 57 become

$$\underline{\phi}_{III} = M_{III}(x)\ a_{III} \tag{59}$$

where the form of $M_{III}(x)$ is given in Eq. 60 in Table 3, and

$$a_{III} = \begin{bmatrix} C_1 \\ C_2 \\ C_3 \\ C_4 \end{bmatrix} \quad . \tag{61}$$

Region IV will be considered an infinite water medium. The diffusion equations in this region are

$$\begin{aligned} D_{1IV}\nabla^2\phi_{1IV} - \Sigma_{1IV}\phi_{1IV} &= 0 \\ D_{2IV}\nabla^2\phi_{2IV} - \Sigma_{2IV}\phi_{2IV} + \Sigma_{1IV}\phi_{1IV} &= 0 \quad . \end{aligned} \tag{62}$$

Table 3. Equation 60

$$M_{III}(x) =$$

$$\begin{bmatrix} \cosh\mu_{1III}x & \sinh\mu_{1III}x & 0 & 0 \\ S_{III}\cosh\mu_{1III}x & S_{III}\sinh\mu_{1III}x & \cosh\mu_{2III}x & \sinh\mu_{2III}x \\ D_{1III}\mu_{1III}\sinh\mu_{1III}x & D_{1III}\mu_{1III}\cosh\mu_{1III}x & 0 & 0 \\ S_{III}D_{2III}\mu_{1III}\sinh\mu_{1III}x & S_{III}D_{2III}\mu_{1III}\cosh\mu_{1III}x & D_{2III}\mu_{2III}\sinh\mu_{2III}x & D_{2III}\mu_{2III}\cosh\mu_{2III}x \end{bmatrix}$$

The solutions of these equations for the infinite medium are

$$\begin{aligned}
\phi_{1IV} &= E_1 e^{-\mathcal{H}_{1IV}x} \\
\phi_{2IV} &= S_{IV}E_1 e^{-\mathcal{H}_{1IV}x} + E_2 e^{-\mathcal{H}_{2IV}x} \\
J_{1IV} &= -D_{1IV}\mathcal{H}_{1IV}E_1 e^{-\mathcal{H}_{1IV}x} \\
J_{2IV} &= -S_{IV}D_{2IV}\mathcal{H}_{1IV}E_1 e^{-\mathcal{H}_{1IV}x} - D_{2IV}\mathcal{H}_{2IV}E_2 e^{-\mathcal{H}_{2IV}x}
\end{aligned} \tag{63}$$

where

$$\begin{aligned}
\mathcal{H}^2_{1IV} &= \frac{\Sigma_{1IV}}{D_{1IV}} = \frac{1}{\tau_{IV}} \\
\mathcal{H}^2_{2IV} &= \frac{\Sigma_{2IV}}{D_{2IV}} = \frac{1}{L^2_{IV}} \\
S_{IV} &= \frac{D_{1IV}}{D_{2IV}\left(\frac{\tau_{IV}}{L^2_{IV}} - 1\right)} \quad .
\end{aligned} \tag{64}$$

In matrix notation Eqs. 63 become

$$\vec{\phi}_{IV} = M_{IV}(x)\ a_{IV} \tag{65}$$

where

$$a_{IV} = \begin{bmatrix} E_1 \\ \\ E_2 \end{bmatrix} \tag{66}$$

$$M_{IV}(x) = \begin{bmatrix} e^{-\mu_{1IV}x} & 0 \\ S_{IV}e^{-\mu_{1IV}x} & e^{-\mu_{2IV}x} \\ -D_{1IV}\mu_{1IV}e^{-\mu_{1IV}x} & 0 \\ -S_{IV}D_{2IV}\mu_{1IV}e^{-\mu_{1IV}x} & -D_{2IV}\mu_{2IV}e^{-\mu_{2IV}x} \end{bmatrix} \tag{67}$$

The requirement of continuity of neutron flux and neutron current at the interfaces of adjacent regions in the reactor gives the following criticality conditions:

$$\begin{aligned} \vec{\phi}_I(x_1) &= \vec{\phi}_{II}(x_1) \\ \vec{\phi}_{II}(x_2) &= \vec{\phi}_{III}(x_2) \\ \vec{\phi}_{III}(x_3) &= \vec{\phi}_{IV}(x_3) \end{aligned} \tag{68}$$

or

$$\begin{aligned} M_I(x_1)a_I &= M_{II}(x_1)a_{II} \\ M_{II}(x_2)a_{II} &= M_{III}(x_2)a_{III} \\ M_{III}(x_3)a_{III} &= M_{IV}(x_3)a_{IV} \end{aligned} \tag{69}$$

.

The matrices a_{II} and a_{III} may be now eliminated from the criticality conditions by the following matrix operations. Both sides of the first equation in 69 are multiplied by the inverse $M_{II}^{-1}(x_1)$ and both sides of the second equation in 69 by the inverse $M_{III}^{-1}(x_2)$ to get

$$a_{II} = M_{II}^{-1}(x_1)M_I(x_1)a_I \tag{70}$$

$$a_{III} = M_{III}^{-1}(x_2)M_{II}(x_2)a_{II} \quad . \tag{70}$$

The substitution of Eqs. 70 into the last of Eqs. 69 now gives

$$M_{IV}(x_3)a_{IV} = M_{III}(x_3)M_{III}^{-1}(x_2)M_{II}(x_2)M_{II}^{-1}(x_1)M_I(x_1)a_I \quad . \tag{71}$$

This criticality condition can be simplified even more by multiplying both sides of Eq. 71 by a matrix Q such that

$$QM_{IV}(x_3) \equiv 0 \quad . \tag{72}$$

It may be verified by substitution that

$$Q = \begin{bmatrix} 1 & 0 & \dfrac{1}{\mathcal{H}_{1IV}D_{1IV}} & 0 \\ 0 & 1 & \dfrac{S_{IV}}{D_{1IV}}\left(\dfrac{1}{\mathcal{H}_{1IV}} - \dfrac{1}{\mathcal{H}_{2IV}}\right) & \dfrac{1}{\mathcal{H}_{2IV}D_{2IV}} \end{bmatrix} \tag{73}$$

Thus the critical equation reduces to the following 2 by 2 critical determinant:

$$\det QM_{III}(x_3)M_{III}^{-1}(x_2)M_{II}(x_2)M_{II}^{-1}(x_1)M_I(x_1) = 0 \quad . \tag{74}$$

The solution of Eq. 74 is greatly simplified if the independent variable x in the above matrices is everywhere replaced by $x - x_o$ where x_o in the matrices of any given region designates the inner boundary of that region. The replacement of x by $x - x_o$ is merely a transformation of the independent variable which has no effect upon the form of the equations. When this substitution is made in Eq. 74 the critical determinant for the UTR-10 without the fission plate becomes

$$\det QM_{III}(t_{III})M_{III}^{-1}(0)M_{II}(t_{II})M_{II}^{-1}(0)M_I(t_I) = 0 \tag{75}$$

where t_i is the thickness of the respective region.

If a thin fission plate loaded with U^{235} is inserted at the graphite-water boundary at x_3 it will act as a plane source of fast neutrons and as a sink for thermal neutrons. This can be illustrated schematically as shown in Fig. 3 where the neutron currents illustrated are based on the normal sign convention. The magnitude of the discontinuity in the curve of fast neutron current at x_3 is equal to the fast neutron source intensity, q_1. Similarly, the discontinuity in the curve of thermal neutron current at x_3 equals the magnitude of the thermal neutron sink, q_2, presented by the fission plate. If it is assumed that the fission plate is very thin, so that the flux in the plate is nearly constant,

$$\begin{aligned} q_1 &= \nu \Sigma_{fp} t_p \phi_2(x_3) \\ q_2 &= \Sigma_{ap} t_p \phi_2(x_3) \end{aligned} \tag{76}$$

where the symbols have all been defined. Therefore, with the fission plate present at the boundary between regions III and IV the boundary conditions there become

$$\begin{aligned} \phi_{1III}(x_3) &= \phi_{1IV}(x_3) \\ \phi_{2III}(x_3) &= \phi_{2IV}(x_3) \\ J_{1III}(x_3) &= J_{1IV}(x_3) + q_1 \\ J_{2III}(x_3) &= J_{2IV}(x_3) - q_2 \end{aligned} \tag{77}$$

where the J's are again the negatives of the usual neutron currents. Now, with the use of Eqs. 63, it is possible to write

$$\begin{aligned} J_{1IV}(x_3) + q_1 = (\nu \Sigma_{fp} t_p S_{IV} - D_{1IV} \mathcal{H}_{1IV}) E_1 e^{-\mathcal{H}_{1IV} x_3} \\ + \nu \Sigma_{fp} t_p E_2 e^{-\mathcal{H}_{2IV} x_3} \end{aligned} \tag{78}$$

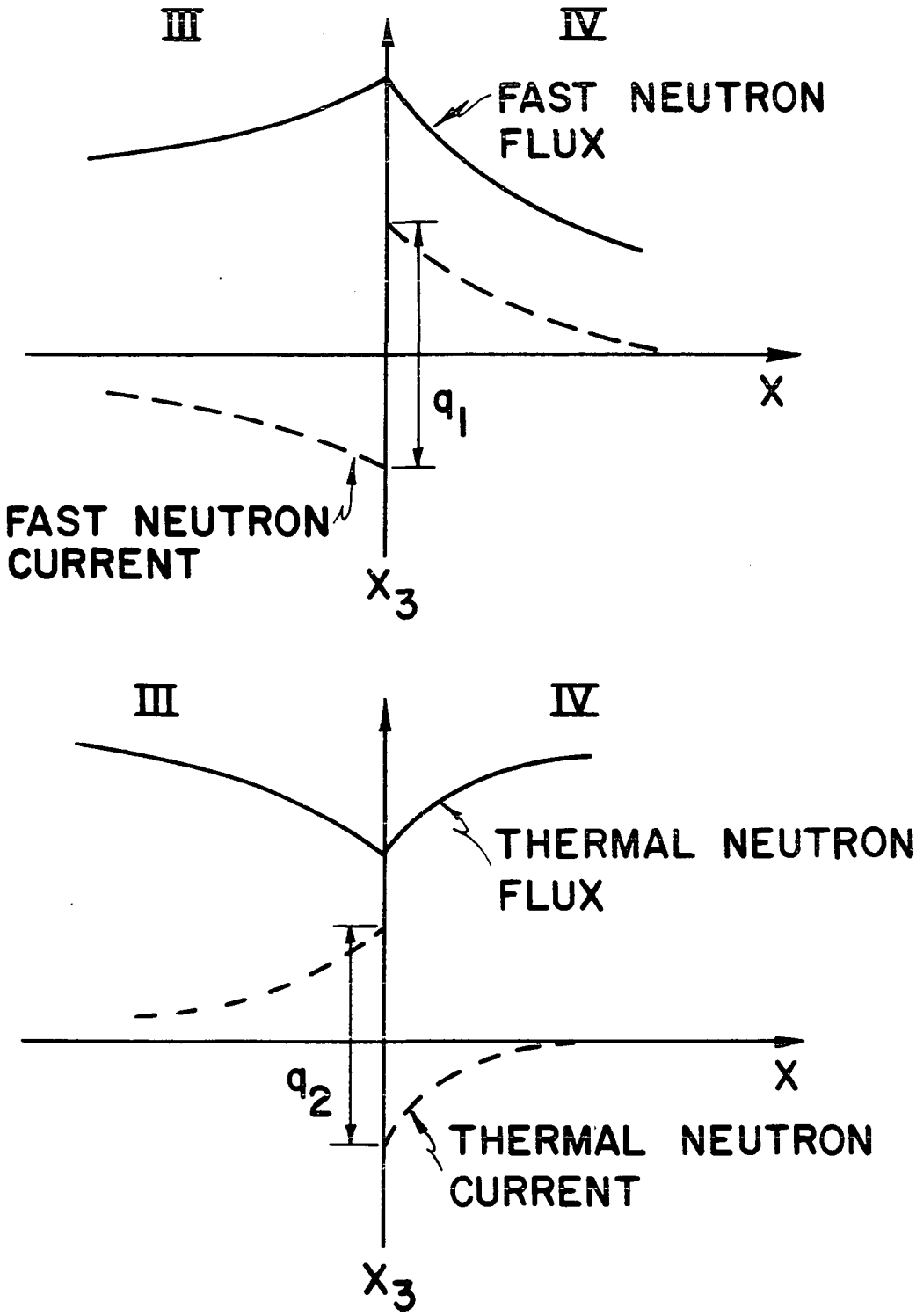

Fig. 3. Schematic representation of neutron flux and net current around fission plate

and

$$J_{2IV}(x_3) - q_2 = -S_{IV}(D_{2IV}\mathcal{H}_{1IV} + \Sigma_{ap}t_p)E_1 e^{-\mathcal{H}_{1IV}x_3} - (D_{2IV}\mathcal{H}_{2IV} + \Sigma_{ap}t_p)E_2 e^{-\mathcal{H}_{2IV}x_3} \quad . \tag{79}$$

If the independent variable x in the above equations is replaced by $x - x_o$ as before, the matrix $M_{IV}(0)$ in the critical equation becomes

$$M'_{IV}(0) = \begin{bmatrix} 1 & 0 \\ S_{IV} & 1 \\ \nu\Sigma_{fp}t_pS_{IV} - D_{1IV}\mathcal{H}_{1IV} & \nu\Sigma_{fp}t_p \\ -S_{IV}(D_{2IV}\mathcal{H}_{1IV} + \Sigma_{ap}t_p) & -(D_{2IV}\mathcal{H}_{2IV} + \Sigma_{ap}t_p) \end{bmatrix} \tag{80}$$

where the prime indicates the matrix applies when the fission plate is present. It may be verified by substitution that the matrix Q' which satisfies the equation $Q'M'_{IV}(0) \equiv 0$ is

$$Q' = \begin{bmatrix} D_{1IV}\mathcal{H}_{1IV} & -\nu\Sigma_{fp}t_p & 1 & 0 \\ S_{IV}D_{2IV}(\mathcal{H}_{1IV} - \mathcal{H}_{2IV}) & D_{2IV}\mathcal{H}_{2IV} + \Sigma_{ap}t_p & 0 & 1 \end{bmatrix} \tag{81}$$

All the other matrices in the critical equation remain the same in both cases. Thus, with the fission plate present at the boundary between regions III and IV the critical determinant becomes

$$\det Q'M_{III}(t_{III})M^{-1}_{III}(0)M_{II}(t_{II})M^{-1}_{II}(0)M_I(t_I) = 0 \tag{82}$$

The inverse matrices in Eqs. 75 and 82 may be found by applying the standard rules of matrix algebra as presented in such texts as Finkbeiner (3). It is thus found that

$$M_{III}^{-1}(0) = \begin{bmatrix} 1 & 0 & 0 & 0 \\ 0 & 0 & \frac{1}{D_{1III}H_{1III}} & 0 \\ -S_{III} & 1 & 0 & 0 \\ 0 & 0 & -\frac{S_{III}}{D_{1III}H_{2III}} & \frac{1}{D_{2III}H_{2III}} \end{bmatrix} . \quad (83)$$

When Eq. 83 is multiplied on the left by $M_{III}(t_{III})$ the matrix $M_{III}(t_{III})M_{III}^{-1}(0)$ is found to have the form shown in Eq. 84 in Table 4. Similarly it is found that $M_{II}(t_{II})M_{II}^{-1}(0)$ has the form shown in Eq. 85 in Table 5.

The next step is to solve the critical determinant in Eq. 75 for the critical loading of U^{235} in the UTR-10 without the fission plate. This involves a trial and error approach to find the determinant whose value is exactly zero. The quantity that is varied in the different trials is the loading of U^{235} in the core of the reactor. This produces changes in the elements of the matrices for region II while the matrices for the other regions will remain the same for all trials.

The nuclear parameters were obtained from Reference 15 and are tabulated in Table 6. The diffusion length, L, and the age τ in the different materials were calculated from the following relations:

$$L^2 = \frac{D_2}{\Sigma_2}$$

$$\tau = \frac{D_1}{\Sigma_1} \quad . \quad (86)$$

Table 4. Equation 84

$$M_{III}(t_{III})M_{III}^{-1}(0) = \begin{bmatrix} M_1 & 0 & \frac{M_3}{D_{1III}\mathcal{H}_{1III}} & 0 \\ S_{III}(M_1-M_2) & M_2 & \frac{S_{III}}{D_{1III}}\left(\frac{M_3}{\mathcal{H}_{1III}} - \frac{M_4}{\mathcal{H}_{2III}}\right) & \frac{M_4}{D_{2III}\mathcal{H}_{2III}} \\ D_{1III}\mathcal{H}_{1III}M_3 & 0 & M_1 & 0 \\ S_{III}D_{2III}(\mathcal{H}_{1III}M_3-\mathcal{H}_{2III}M_4) & D_{2III}\mathcal{H}_{2III}M_4 & S_{III}\frac{D_{2III}}{D_{1III}}(M_1-M_2) & M_2 \end{bmatrix}$$

$$M_1 = \cosh \mathcal{H}_{1III}t_{III} \qquad M_3 = \sinh \mathcal{H}_{1III}t_{III}$$

$$M_2 = \cosh \mathcal{H}_{2III}t_{III} \qquad M_4 = \sinh \mathcal{H}_{2III}t_{III}$$

Table 5. Equation 85

$$M_{II}(t_{II})M_{II}^{-1}(0)$$

$$= \frac{1}{S_{1II}-S_{2II}} \begin{bmatrix} N_4S_{1II}-N_2S_{2II} & N_2-N_4 & \frac{N_3S_{1II}}{D_{1II}m} - \frac{N_1S_{2II}}{D_{1II}\ell} & \frac{N_1}{D_{2II}\ell} - \frac{N_3}{D_{2II}m} \\ N_4S_{1II}S_{2II}-N_2S_{1II}S_{2II} & N_2S_{1II}-N_4S_{2II} & \frac{N_3S_{1II}S_{2II}}{D_{1II}m} - \frac{N_1S_{1II}S_{2II}}{D_{1II}\ell} & \frac{N_1S_{1II}}{D_{2II}\ell} - \frac{N_3S_{2II}}{D_{2II}m} \\ D_{1II}(N_1\ell S_{2II}+N_3mS_{1II}) & -D_{1II}(N_1\ell+N_3m) & N_4S_{1II}-N_2S_{2II} & \frac{D_{1II}}{D_{2II}}(N_2-N_4) \\ D_{2II}S_{1II}S_{2II}(N_1\ell+N_3m) & -D_{2II}(N_1\ell S_{1II}+N_3mS_{2II}) & \frac{D_{2II}}{D_{1II}}S_{1II}S_{2II}(N_4-N_2) & N_2S_{1II}-N_4S_{2II} \end{bmatrix}$$

$$N_1 = \sin \ell t_{II} \qquad N_3 = \sinh mt_{II}$$

$$N_2 = \cos \ell t_{II} \qquad N_4 = \cosh mt_{II}$$

Table 6. Nuclear parameters for two-group diffusion theory

Material	Σ_2 (cm^{-1})	Σ_{tr2} (cm^{-1})	D_2 (cm)	Σ_f (cm^{-1})	Σ_{tr1} (cm^{-1})	D_1 (cm)	Σ_1 (cm^{-1})
H_2O	0.0197	2.08	0.160	0	0.28	1.19	0.036
Al	0.01228	0.084	3.97	0	0.236	1.41	0
U^{235}	28.51	0.497	0.670	24.10	0.497	0.67	0
C	0.00036	0.369	0.903	0	0.303	1.10	0.00314

Since the disadvantage factor $\frac{\bar{\phi}\ \text{moderator}}{\bar{\phi}\ \text{fuel}}$ is nearly unity in the UTR-10, the core may be treated as a homogeneous medium and the average macroscopic neutron cross sections for the core may be found from

$$\bar{\Sigma} = \sum_i f_i N_i \sigma_i = \sum_i f_i \Sigma_i \tag{87}$$

where f_i is the volume fraction of the i-th constituent. The volume fractions for the core were calculated from the dimensions given in Reference 16 and are as follows:

$$\begin{aligned} f_{H_2O} &= 0.820338 \\ f_{Al} &= 0.179662 - 0.0012178\ W_{25} \\ f_{U^{235}} &= 0.0012178\ W_{25} \end{aligned} \tag{88}$$

where W_{25} is the mass in kg of U^{235} in one core tank of the UTR-10. The small amount of U^{238} in the fuel may be ignored in these calculations. When the volume fractions from Eq. 88 are substituted in Eq. 87 along with the appropriate Σ_i's, the following equations are obtained:

$$\begin{aligned}
\bar{\Sigma}_{2II} &= 0.0183669 + 0.0347045\ W_{25} \\
\bar{\Sigma}_{fII} &= 0.0293490\ W_{25} \\
\bar{\Sigma}_{tr2II} &= 1.721395 + 0.0005030\ W_{25} \\
\bar{\Sigma}_{1II} &= 0.0295322 \\
\bar{\Sigma}_{tr1II} &= 0.2720949 + 0.0003178458\ W_{25} \ .
\end{aligned} \tag{89}$$

These average values of the macroscopic neutron cross sections may now be used to calculate the diffusion coefficients, D_{2II} and D_{1II}, the diffusion length, L_{II}, and the age, τ_{II}, in the theoretically homogenized core which makes up region II:

$$\begin{aligned}
D_{2II} &= \frac{1}{3\bar{\Sigma}_{tr2II}} = \frac{1}{5.164185 + 0.001509\ W_{25}} \\
D_{1II} &= \frac{1}{3\bar{\Sigma}_{tr1II}} = \frac{1}{0.8162847 + 0.0009535374\ W_{25}} \\
L^2_{II} &= \frac{D_{2II}}{\bar{\Sigma}_{2II}} = \frac{1}{0.0948501 + 0.1792482\ W_{25} + 0.00005237\ W^2_{25}} \\
\tau_{II} &= \frac{D_{1II}}{\bar{\Sigma}_{1II}} = \frac{1}{0.0241067 + 0.0000281601\ W_{25}}
\end{aligned} \tag{90}$$

Since the critical equations were developed for a one-dimensional infinite slab reactor, the neutron leakage from the sides of the finite UTR-10 must also be taken into account. This is done in regions I and III by using an effective reciprocal relaxation length, $\bar{H}$, for the finite medium in place of the infinite medium, H, defined in the derivation. The quantity $\bar{H}^2$ is found by adding the buckling in the y and z directions to the corresponding infinite medium H^2. Thus

$$\begin{aligned}
\bar{M}^2_{1I} &= M^2_{1I} + B^2_I \\
\bar{M}^2_{2I} &= M^2_{2I} + B^2_I \\
\bar{M}^2_{1III} &= M^2_{1III} + B^2_{III} \\
\bar{M}^2_{2III} &= M^2_{2III} + B^2_{III}
\end{aligned} \tag{91}$$

where $B^2_I = 0.0013623\ cm^{-2}$ and $B^2_{III} = 0.0019668\ cm^{-2}$. The water tank that makes up region IV may be considered an infinite medium for neutrons since both the neutron diffusion length and slowing down length in water are small compared to the dimensions of the water tank. Thus no correction is needed in this region. In the matrices for region II $\bar{\ell}$ is used for the finite medium in place of ℓ and $\bar{m}$ in place of m everywhere except in the calculation of the coupling constants S_{1II} and S_{2II} where the original ℓ^2 is used. The quantities $\bar{\ell}$ and $\bar{m}$ are found from the following relations given by Spinrad and Kurath (19):

$$\begin{aligned}
\bar{\ell}^2 &= \ell^2 - B^2_{II} \\
\bar{m}^2 &= m^2 + B^2_{II}
\end{aligned} \tag{92}$$

where $B^2_{II} = 0.003567617\ cm^{-2}$. The term B^2_{II} was calculated from the equivalent bare core dimensions obtained by using the reflector savings for the UTR-10 given by Nowak and Chow (15, p. 7).

The trial and error solution of Eq. 75 is now greatly facilitated by setting up calculation sheets for each region similar to those outlined by Spinrad and Kurath (19). The calculations outlined are then carried out step by step on these calculation sheets and the matrix for each

region obtained. In region II, k_∞ is calculated for a trial value of fuel loading from the relation

$$k_\infty = \frac{\nu \bar{\Sigma}_{fII}}{\bar{\Sigma}_{2II}} \tag{93}$$

where $\nu = 2.46$. The quantity ℓ^2 for this fuel loading is then obtained as the positive root of Eq. 50 and this value is used in the rest of the calculations for region II. When the matrices from the different calculation sheets are multiplied together according to Eq. 75, the 2 by 2 determinant for that trial calculation is obtained. Several trial values of the determinant in Eq. 75 were calculated by the procedure outlined and were plotted vs. fuel loading as shown in Fig. 4. The critical fuel loading at which the determinant vanishes was then determined from the point at which the curve crosses the abscissa. This theoretical value for the critical fuel loading is 1.08820 kg in each core tank or a total of 2.17640 kg of U^{235}. The actual critical fuel loading as determined by the approach to critical experiment when the fuel was originally loaded in the UTR-10 is approximately 2.922 kg.

The difference between the theoretical and actual values for the critical fuel loading may be caused by a combination of reasons. The actual critical loading was determined with the control rods in their position of maximum withdrawal. However, in this position they are located in the reflector just above the active fuel region and would still be exerting a small negative reactivity effect on the reactor. In the theoretical calculations it was assumed that no control rods were present. Also in the theoretical calculations the small poison effect produced by

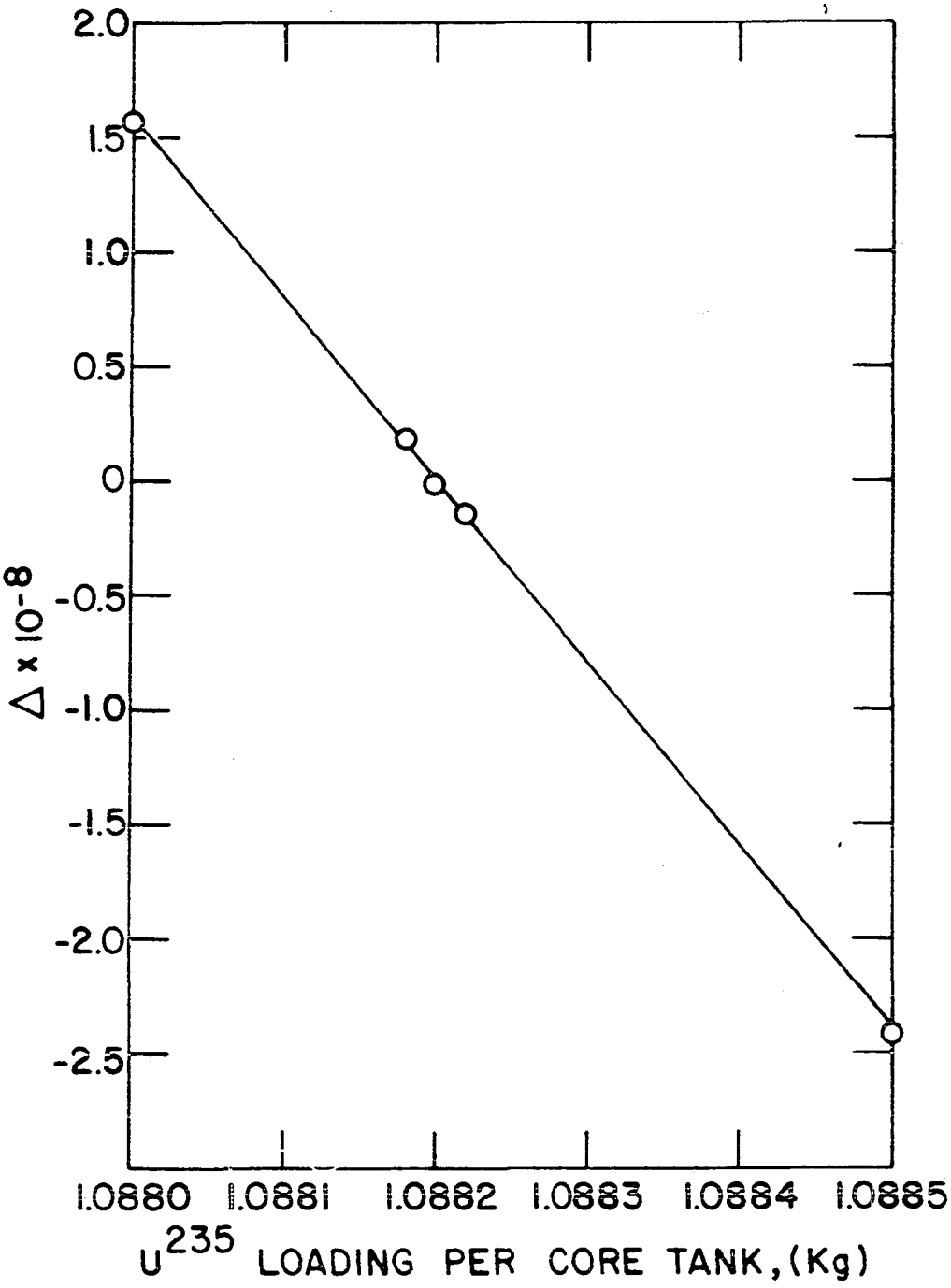

Fig. 4. Trial values of critical determinant, Δ, vs. U^{235} loading per core tank

the U^{238} in the highly enriched uranium was assumed to be negligible.

The results of the theoretical calculations are on the safe side since they indicate that the fuel loading should be less than the actual loading required. If the same parameters are used in the solution of the critical equation for the system including the fission plate, the results obtained for the reactivity effect of the fission plate will also be on the safe side. Therefore, the value 1.08820 kg of U^{235} was used for the fuel loading in Eq. 82 for the system with the fission plate, and this equation was solved by a similar trial and error method using different trial values of ν in the matrix $M_{II}(t_{II})M_{II}^{-1}(0)$. The results of these calculations are shown in Fig. 5 plotted vs. the change in ν from the original value of 2.46. This curve indicates that a fictitious $\Delta\nu$ of about -0.62×10^{-5} would be necessary to maintain the just critical condition when the fission plate is added to the system. When this value is substituted into Eq. 39, the reactivity change produced in the reactor by the fission plate is found to be

$$\Delta\rho = -\frac{\Delta\nu}{\nu} = -\frac{-0.62 \times 10^{-5}}{2.46} = 2.52 \times 10^{-6}\,\frac{\Delta k}{k} \quad . \tag{94}$$

The evaluation of the 2 by 2 determinants in this calculation involves finding the difference between two large nearly equal numbers. Therefore the calculations for this dissertation were carried out to ten significant figures on a Monromatic desk calculator. There may be some question of the validity of this procedure since the data fed into the calculations were only known to two or three significant figures in many cases. However, these data (the nuclear parameters and physical dimensions) were the same for both calculations. The only changes made between

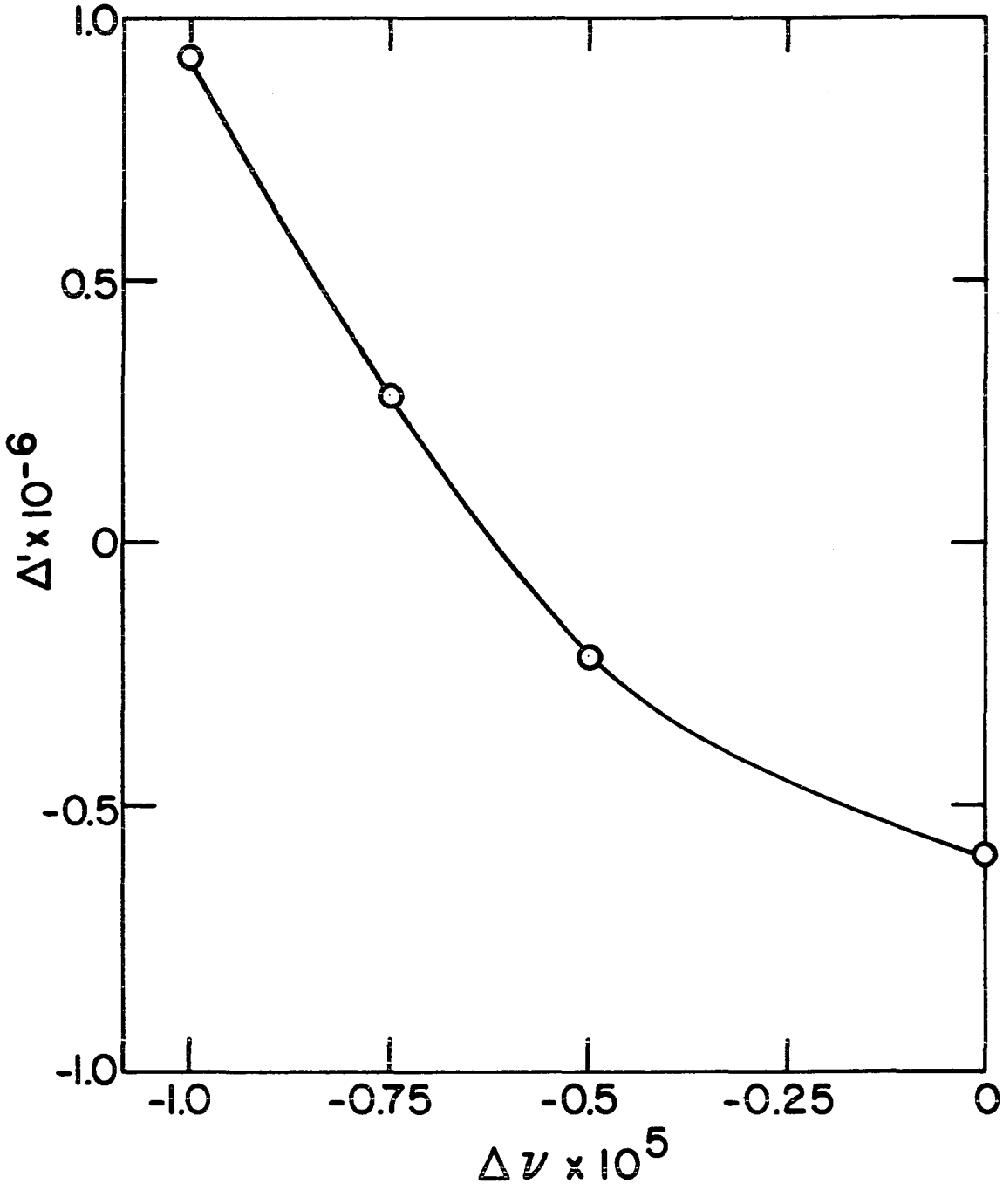

Fig. 5. Trial values of critical determinant with fission plate, Δ', vs. change in ν, $\Delta\nu$, in core matrix

the two calculations were the addition of the fission plate and the change in ν to just balance the effect of the fission plate. Since we are only interested in the change in ν and the other data may be considered constants of the system, it is felt that carrying the calculations out to ten significant figures was justified.

An Analogy between the Increased Neutron Flux at the Core Boundary and a Hypothetical Increase in the Nonleakage Probability

A rough estimate of the reactivity effect produced by the fission plate may be obtained quickly and easily from an analogy between the increased neutron flux at the core boundary and a hypothetical increase in the nonleakage probability to produce the same effect. Let ϕ denote the thermal neutron flux at the north edge of the north core tank (Fig. 1) and let ϕ' be the thermal neutron flux at that point with the fission plate present. Then from Eq. 23 it is found that the thermal flux at the surface of the north core tank is increased by the factor 1.000072 when the fission plate is added to the system so that

$$\phi' = 1.000072\ \phi \quad . \tag{95}$$

Now consider the well known equation for the effective multiplication factor in a finite multiplying medium,

$$k_{eff} = \frac{k_\infty e^{-B^2\tau}}{1 + B^2L^2} = \mathcal{L}\, k_\infty , \tag{96}$$

where $\mathcal{L}$ is the nonleakage probability for both fast and thermal neutrons. With the fission plate present, as indicated by the primes, one

may write

$$k'_{eff} = \mathcal{L}' k_{\infty} = \frac{\mathcal{L}'}{\mathcal{L}} k_{eff} \quad . \tag{97}$$

Since the increase in the flux in Eq. 95 is due to neutrons returning to the core from the fission plate source, an analogy may be drawn between this increase and the change in the nonleakage factor in Eq. 97. However, the presence of the fission plate materially affects only the leakage from the north face of the core, and the leakage from the other faces is essentially unchanged. For the UTR-10 the total reflector savings, as given by Nowak and Chow (15, p. 7), are 5.5 in. in the vertical direction and 10.2 in. in the horizontal direction. When these values are used along with the physical dimensions of the core given in Fig. 1, it is found that the north face represents approximately 1/8 of the equivalent bare core surface. Therefore, according to this analogy, the overall nonleakage probability is increased by about $1 + \frac{0.000072}{8} = 1.000009$. This produces the following change in k_{eff}:

$$\begin{aligned} k'_{eff} - k_{eff} &= (\mathcal{L}' - \mathcal{L}) k_{\infty} \\ &= (1.000009 - 1) \mathcal{L} k_{\infty} \\ &= 9 \times 10^{-6} k_{eff}. \end{aligned} \tag{98}$$

The change in reactivity produced by the fission plate is then given by

$$\Delta\rho = \frac{k'_{eff} - k_{eff}}{k_{eff}} = 9 \times 10^{-6} \frac{\Delta k}{k} \quad . \tag{99}$$

This method gives a somewhat larger value for the reactivity change produced by the fission plate than the values obtained from the two methods discussed above. However, it should be kept in mind that this method is presented only as a way of quickly obtaining a rough estimate

of the reactivity effect of the fission plate. The core geometry of the UTR-10, with the two water moderated fuel regions separated by a graphite internal reflector, makes it especially difficult to get good results from this method since the neutron leakage is not uniform over the surface of the core. For this reason the value of 1/8 used above is only a crude approximation for the relation between the change in the nonleakage probability caused by the fission plate and an equivalent change in the overall nonleakage probability.

FISSION PLATE POWER AND SHIELDING REQUIREMENTS

The next step is to determine the maximum fission rate in the fission plate and to determine whether or not additional shielding is needed around the shield tank to attenuate the radiation produced in the fission plate to a safe level. It will again be assumed that the multiplication of the thermal neutron flux at the plate position produced by the fission plate is two. Since the fuel plates that are to be used to make up the fission plate have a very light loading of U^{235}, it will also be assumed that there is no flux depression in the plate. Then the fission rate per cm^2, $R_{f\ max.}$, produced at the center of the fission plate is

$$R_{f\ max.} = 2N_p^{25}\sigma_f^{25}\phi_s(0) \tag{100}$$

where the symbols are defined the same as before.

The quantity $\phi_s(0)$ may be calculated from Eq. 32 and is found to be 6.885×10^{-3} thermal neutrons per cm^2 per sec per unit thermal flux at the surface of the core tank. According to Nowak and Chow (15), the thermal neutron flux at the surface of the core tank is about 8.3×10^{10} neutrons per cm^2 per sec when the reactor is at full power of 10 kw. When these values are used $\phi_s(0)$ at full reactor power is found to be 5.71×10^8 thermal neutrons per cm^2 per sec and $R_{f\ max.}$ is found to be 1.67×10^8 fissions per cm^2 per sec. If a cosine distribution of neutron flux in the y and z directions going to zero at the extrapolated dimensions of the graphite duct is assumed, the total fission rate for a 24 in. square active plate area is

$$R_{f\ total} = R_{f\ max} \int_{-30.48}^{30.48} \int_{-30.48}^{30.48} \cos\frac{\pi y}{100} \cos\frac{\pi z}{100}\, dydz \qquad (101)$$

$$= 4.525 \times 10^{11} \text{ fissions/sec.}$$

If the average energy produced per fission is assumed to be 190 Mev, this fission rate is found to be equal to a power of 13.71 watts.

This power level should cause no heating problems in the fission plate since it will be cooled by natural convection in the shield tank water and by conduction through its aluminum support structure. Even if the fission plate was completely thermally insulated from its surroundings this power would cause a heating rate of only 21.6 F per hour.

However, when the reactor is operating at full power the fission plate will be a very intense source of nuclear radiations, both neutrons and gammas. The procedure used in the calculation of the shielding required to attenuate this radiation is that outlined by Glasstone and Sesonske (8). The maximum dose rate at the surface of the existing shield produced by the fission plate will be calculated first, and if this is above permissible levels the additional shielding required will be determined. The calculations are divided into three sections according to types of radiation considered: 1) primary gammas originating in the fission plate, 2) fast neutrons produced by the fission process, and 3) secondary gammas produced by neutron absorption in the water. A scale drawing of a horizontal section through the concrete shield and the shield tank at the mid-height of the fission plate is shown in Fig. 6. The dose rates are calculated for the points indicated as P_1, P_2, and P_3 and also for a point P_4 at the surface of the water directly above the fission plate. To

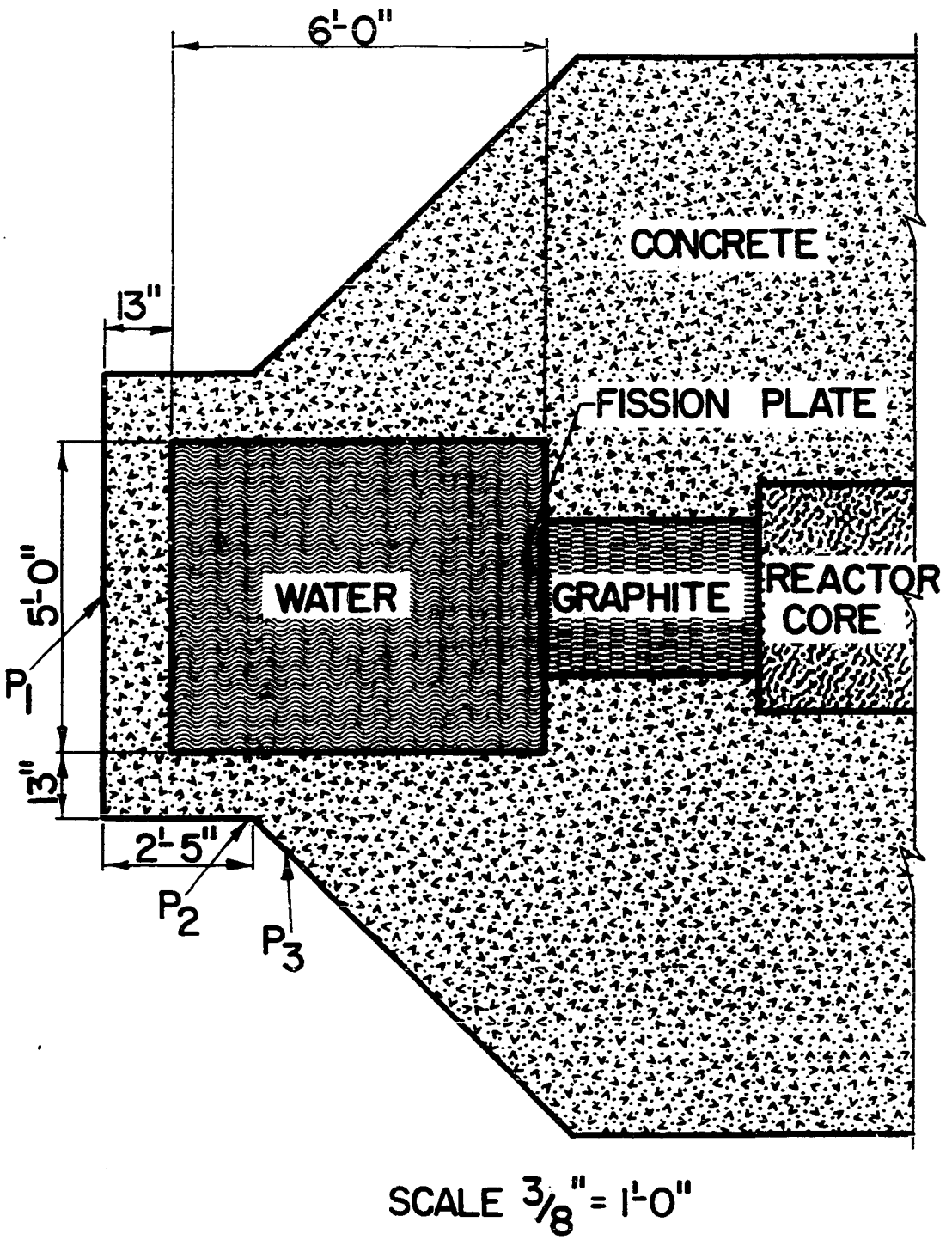

Fig. 6. Sectional view of concrete shield and shield tank showing points for which surface dose rates were calculated

simplify the calculations, the fission plate is considered a point source in these calculations. The errors involved in such an approximation are tabulated for various geometries by Rockwell (18, p. 411). The maximum error produced in these calculations is about 10 per cent and is in the safe direction.

Since the primary gammas have a considerable range of energies, and since the attenuation coefficient for gamma rays is energy dependent, the calculations are simplified by dividing the energy spectrum into four groups. The photons in each group are assumed to be monoenergetic with energies of 1, 2, 4, and 6 Mev respectively as suggested in Glasstone and Sesonske (8). The gamma energy flux $\phi_\gamma(t)$ at the surface of the shield due to each group of gammas is then calculated from the following equation,

$$\phi_\gamma(t) = \frac{B(\mu t)\, S_\gamma e^{-\mu t}}{4\pi t^2} \tag{102}$$

where

$B(\mu t)$ = energy-flux buildup factor as a function of μt

μ = linear attenuation coefficient

t = total thickness of shield

$\mu t = \mu_1 t_1 + \mu_2 t_2$ where subscripts 1 and 2 stand for water and concrete respectively

S_γ = gamma energy source strength determined by the fission rate in the fission plate.

This energy flux is then converted to dose rate in mrem per hour. Data

to be used in these calculations are listed in Table 7. The buildup factors are given in Table 10.2 of Glasstone and Sesonske (8, p. 575).

Table 7. Data for gamma shielding calculation

Property	Group I	Group II	Group III	Group IV
Average photon energy, Mev	1	2	4	6
Prompt fission, Mev per fission	3.45	3.09	1.04	0.26
Fission products, Mev per fission	5.16	1.74	0.32	--
Mev per neutron capture in water	--	2.2	--	--
μ in water, cm^{-1}	0.0706	0.0493	0.0339	0.0273
μ in concrete, cm^{-1}	0.149	0.105	0.0745	0.0630
μ in lead, cm^{-1}	0.776	0.518	0.476	0.494
μ in iron, cm^{-1}	0.468	0.333	0.259	0.239
Conversion factor from energy flux to dose rate, $\frac{Mev/(cm^2)(sec)}{mrem/hr}$	520	620	800	910

For fast neutron attenuation in water Glasstone and Sesonske (8, p. 586) recommend the point kernel G(R) represented by the sum of two exponential terms, which allow for the buildup factor,

$$G(R) = \frac{1}{4\pi R^2}\left[Ae^{-aR} + (1 - A)e^{-bR}\right] . \qquad (103)$$

The values of the constants A, a, and b, derived from measurements in water are

$$A = 0.892, \qquad a = 0.129, \qquad b = 0.091.$$

An exponential attenuation of the fast neutrons in the concrete wall of the tank is used where the fast neutron relaxation length is 12 cm as given by Reference 8, p. 578. Thus the fast neutron flux $\phi(t)$ at the surface of the shield is given by

$$\phi(t) = \frac{S_n}{4\pi t^2}\left[Ae^{-at_1} + (1 - A)e^{-bt_1}\right] e^{-t_2/12} \qquad (104)$$

where the fast neutron source strength equals 2.46 times the fission rate in the plate. The fast neutron flux at the surface of the shield calculated from Eq. 104 is converted to an equivalent dose rate by the conversion factor 7 $\frac{\text{neutrons}/(\text{cm}^2)(\text{sec})}{\text{mrem/hr}}$ given in Reference 8, p. 528.

In the calculation of the dose rate due to secondary gammas an approximate method suggested by Glasstone (6) is used. In this method it is postulated that all the fast neutrons entering the shield are captured at a distance within the shield equal to τ/λ called the "age displacement", where τ is the Fermi age of thermal neutrons in the shield material and λ is the relaxation length for fast neutrons in the shield. Thus the effective shield thickness for the secondary gammas is $t' = t - \frac{\tau}{\lambda}$. When the value of λ for water given in Reference 8, p.578, is used, τ/λ is found to be 3.3 cm. Equation 102 with t' substituted for t is then used to determine the energy flux at the surface of the shield. The only secondary gammas that need to be considered here are the 2.2 Mev gammas produced by neutron absorption in the hydrogen in the water.

The dose rates at points P_1, P_2, P_3, and P_4 produced by radiation from the fission plate when operated at full power are tabulated in

Table 8. As can be seen in the table, the dose rate at the surface produced by the fission plate alone is above the maximum permissible level of 2.5 mrem/hr for a 40 hr work week at 3 of the 4 points checked. Also the gamma dose rate at P_1 without the fission plate has been measured at 12 mrem/hr when the reactor was at full power. Thus the total maximum dose rate at P_1 with the fission plate would be about 14.76 mrem/hr. Since normally the facility will only be used for a few hours a week these dose rates could be tolerated if careful radiation monitoring is carried out and strict time limits in high dose areas are imposed. However, two inches of lead or four inches of iron added to the surface of the shield tank would reduce the total dose rate at P_1 to about two mrem/hr or 2.7 mrem/hr respectively.

Table 8. Maximum dose rates due to the fission plate (mrem/hr)

Source	P_1	P_2	P_3	P_4
Primary gammas	2.519	4.667	2.850	1.450
Fast neutrons	0.0001	0.006	0.008	0.000
Secondary gammas	0.239	0.537	0.281	0.115
Total	2.758	5.210	3.139	1.565

These calculations have all been based on the theoretical design value of 5.71×10^8 thermal neutrons per cm^2 per sec for $\phi_s(0)$ at the center of the proposed fission plate position in the shield tank when the reactor is at full power. This flux has also been measured experimentally

by irradiating gold foils at the desired position and then measuring their induced radioactivity in a calibrated gas flow counting system. The experimental value of $\phi_s(0)$ with the reactor at full power of 10 kw was found to be 3.10×10^8 thermal neutrons per cm^2 per sec. If this experimental value for $\phi_s(0)$ was used in the calculations for the fission plate power and shielding requirements, the power level and the radiation dose rates determined above would be reduced by the factor 0.543.

The difference between the calculated value of $\phi_s(0)$ and the measured value results from the assumptions that were made in the theoretical calculations. These assumptions were purposely made so that the theoretical results would be on the safe side as is indicated by the values of $\phi_s(0)$. The most important factor contributing to the large calculated value for $\phi_s(0)$ was the exaggeration of the extrapolated dimensions of the graphite duct.

FABRICATION AND INSTALLATION OF THE FISSION PLATE

A sectional view of the proposed fission plate assembly for the UTR-10 is shown in Fig. 7. The fission plate proper is made up of 16 UTR-10 fuel plates arranged in two layers as shown. Since the fuel matrix in the plates does not extend all the way to the edge of the plates, the plates in the two layers are arranged so the edges overlap 3/4 in. to insure at least one layer of U^{235} throughout the active fission plate area. A boral diaphragm 1/8 in. by 32 in. by 32 in. with a 22-in. diameter hole is centered over the reactor side of this array of fuel plates to confine the fission reaction to a circle in the center of the fission plate. The diaphragm thus simplifies the source geometry for experiments and eliminates the problem of uneven fuel loading near the edges of the plate. The boral also prevents thermal neutrons from the reactor from streaming around the edges of the fission plate. The hole in the boral diaphragm is filled with an aluminum window welded to the boral sheet. The shield tank side of the fuel plates is covered by a 1/8 in. aluminum cover plate and the whole assembly is placed in an aluminum frame which also acts as a spacer to hold the fuel plates in position. The boral diaphragm and aluminum cover plate are welded to the aluminum frame. All welds are water tight.

The proposed fission plate installation in the UTR-10 shield tank is shown in a sectional view in Fig. 8. To conserve the uranium and minimize the buildup of radioactive fission products in the plate when it is not in use, provisions are made so that the plate may be raised out of the thermal neutron beam emerging from the graphite shield tank duct.

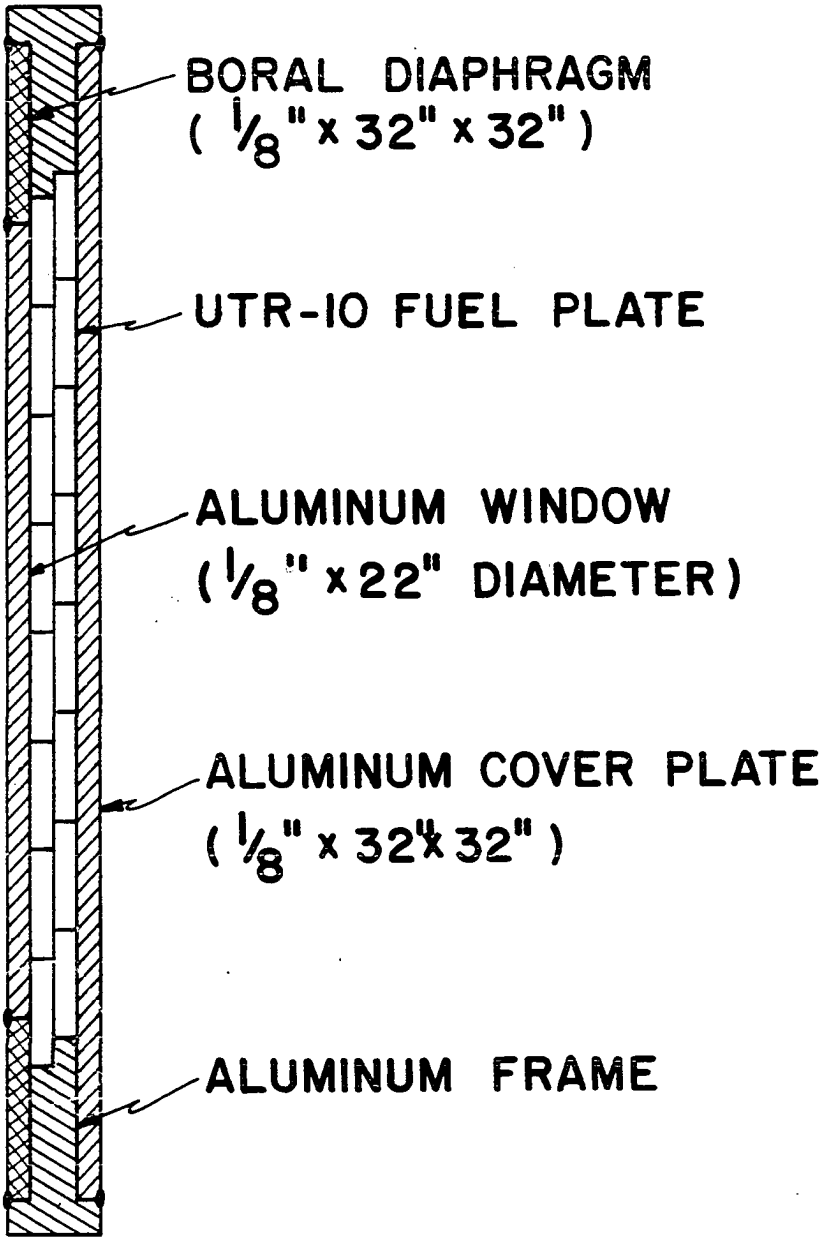

Fig. 7. Sectional view of proposed fission plate assembly for UTR-10 (not to scale)

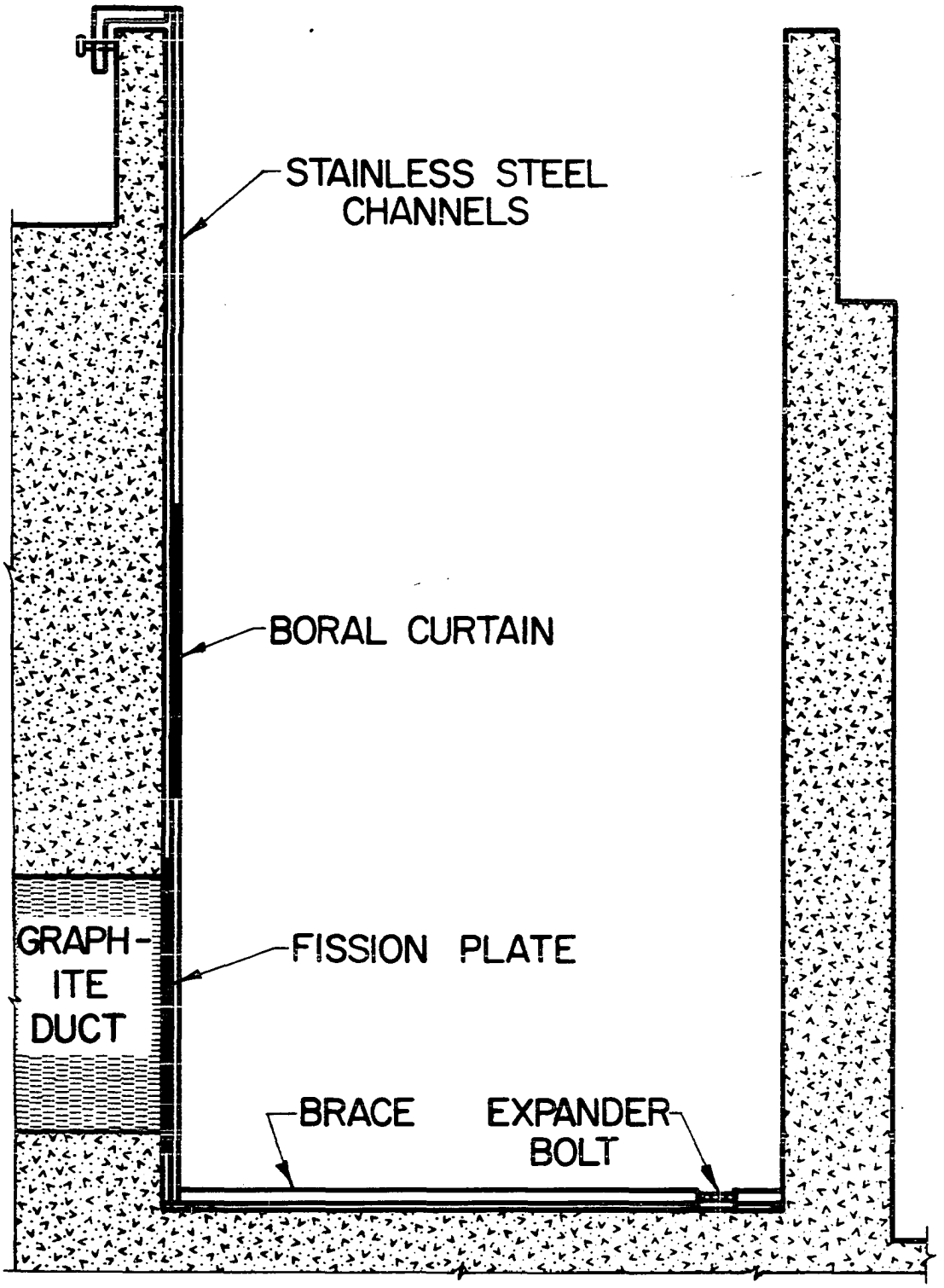

Fig. 8. Sectional view of UTR-10 shield tank showing proposed fission plate installation

To minimize corrosion problems, stainless steel guide channels are used to hold the fission plate in place in the shield tank. Stainless steel cables connected to a small hand operated winch at the top of the tank are used to raise and lower the plate. The guide channels are mounted in the shield tank by means of a C clamp arrangement at the top of the tank wall and a brace rod incorporating an expander bolt running the length of the tank at the bottom. Power changes in the fission plate due to neutron reflection from shielding specimens are eliminated by a 1/8 in. boral curtain which may be positioned on the shield tank side of the fission plate by a second set of stainless steel cables and guide channels.

CONCLUSIONS

The above calculations show that the proposed UTR-10 fission plate installation will present no nuclear control problems. The effective multiplication factor for the fission plate in its graphite-water system was found to be approximately 0.15 indicating that it will be subcritical. The effect of the fission plate on the reactivity of the reactor system was calculated by three methods. The values $1.657 \times 10^{-6} \frac{\Delta k}{k}$ obtained by perturbation theory and $2.52 \times 10^{-6} \frac{\Delta k}{k}$ obtained from 2-group diffusion theory agree within a factor of 1.52. The third method of calculation used, which is only an approximate method and not considered to be as accurate as the other two, yields a value of $9 \times 10^{-6} \frac{\Delta k}{k}$ for the reactivity effect of the fission plate on the reactor system. However, even the quantity $9 \times 10^{-6} \frac{\Delta k}{k}$ is almost a negligible increase in the total reactivity of the system and will present no control problem.

The maximum power level of the fission plate was calculated to be 13.71 watts. This calculation was made for the bare fission plate consisting of the 16 UTR-10 fuel plates. The boral diaphragm and aluminum window in the proposed fission plate assembly will reduce this maximum power by a factor of 0.729. This indicates that a power level of about 10 watts may be expected in the proposed fission plate. This power is adequate to make it a useful fission neutron source for research work. However, a fission plate of this power will increase the radiation dose rate at the outer surface of the shield tank by about 4 mrem per hr at the worst point. Since the dose rate at the surface of the shield tank with the reactor at full power is already 12 mrem per hr, careful

radiation monitoring around the facility will be required and strict time limits in high dose areas must be enforced.

SUGGESTIONS FOR FURTHER STUDY

The work presented here is only the first step in the development of a useful fission plate installation for research work. The actual strength of the fission source is of fundamental importance when absolute results are desired from research conducted with it. Since the actual power level of the fission plate will be quite sensitive to the exact positioning in the shield tank, its power level must be calibrated experimentally after it has been built up and installed in the UTR-10 shield tank. Otis (17) and Morgan et al. (12) discuss several methods that were used at Oak Ridge National Laboratory and Battelle Memorial Institute to calibrate their fission plates.

In order to obtain reliable data from the facility it will be desirable to develop special instrumentation and measuring techniques. Instruments must be designed to measure fast and slow neutron fluxes or dose rates and gamma doses over a wide range of intensities. Cady (2) discusses the instrumentation and calibration procedures used at the LTSF at Oak Ridge.

A third suggestion for further study is to investigate the modification of the facility so that it could be used as a gamma source only. If the fission plate is replaced by a sheet of material such as cadmium with a large (n, γ) cross section an intense plane source of gamma rays would be obtained with practically no neutron contamination. Various materials could be used for the (n, γ) source to obtain various energy gammas.

LITERATURE CITED

1. Bourgeois, J., Lafore, P., Millet, J. P., Rastoin, J., and de Vathaire, F. Methods and experimental coefficients used in reactor shielding calculations. United Nations International Conference on the Peaceful Uses of Atomic Energy, 2nd, Geneva, 1958, Proceedings 13:31-41. 1958.

2. Cady, D. W. The lid tank shielding facility at Oak Ridge National Laboratory. III. Instrumentation. U. S. Atomic Energy Commission Report ORNL-2587 [Oak Ridge National Laboratory, Oak Ridge, Tenn.]. 1960.

3. Finkbeiner, Daniel T., II. Introduction to matrices and linear transformation. San Francisco, Calif., W. H. Freeman and Co. c1960.

4. Galanin, A. D. The theory of thermal-neutron nuclear reactors. Soviet Journal of Atomic Energy Supplement. New York, N. Y., Consultant's Bureau, Inc. c1958.

5. Garabedian, H. L. and Householder, A. S. Multi-group, multi-reflector pile theory. U. S. Atomic Energy Commission Report MonP-246 [Clinton Laboratories, Oak Ridge, Tenn.]. 1947.

6. Glasstone, Samuel. Principles of nuclear reactor engineering. Princeton, N. J., D. Van Nostrand Co., In. 1955.

7. Glasstone, Samuel and Edlund, Milton C. The elements of nuclear reactor theory. Princeton, N. J., D. Van Nostrand Co., Inc. 1952.

8. Glasstone, Samuel and Sesonske, Alexander. Nuclear reactor engineering. Princeton, N. J., D. Van Nostrand Co., Inc. 1963.

9. Goldstein, Herbert. Fundamental aspects of reactor shielding. Reading, Mass., Addison-Wesley Publishing Co., Inc. 1959.

10. Hughes, Donald J., and Schwartz, Robert B. Neutron cross sections. U. S. Atomic Energy Commission Report BNL-325 [Brookhaven National Laboratory, Upton, N. Y.]. 1958.

11. Hwang, Richard N. A theoretical analysis for fission plate in a graphite-water system. Unpublished original manuscript. Ames, Iowa, Department of Nuclear Engineering, Iowa State University of Science and Technology. 1960.

12. Morgan, Walter R., Epstein, Harold M., Anno, James N., Jr., and Chastain, Joel W., Jr. Shielding-research area at Battelle. U. S. Atomic Energy Commission Report BMI-1291 [Battelle Memorial Institute, Columbus 1, Ohio]. 1958.

13. Murray, Raymond L. Nuclear reactor physics. Englewood Cliffs, N. J., Prentice-Hall, Inc. c1957.

14. Nowak, Michael J. Transmission of neutron flux through graphite ducts. U. S. Atomic Energy Commission Report ASAE-11 [American-Standard. Atomic Energy Div., Redwood City, Calif.]. 1957.

15. Nowak, Michael J. and Chow, Ken T. Reactor physics of UTR-10. U. S. Atomic Energy Commission Report ASAE-19 [American-Standard. Atomic Energy Div., Redwood City, Calif.]. 1957.

16. Operating manual for the Iowa State University UTR-10 reactor. U. S. Atomic Energy Commission Report ATL-136 [Advanced Technology Laboratories Division of American-Standard, Mountain View, Calif.]. 1959.

17. Otis, D. R. The lid tank shielding facility at Oak Ridge National Laboratory. II. U. S. Atomic Energy Commission Report ORNL-2350 [Oak Ridge National Laboratory, Oak Ridge, Tenn.]. 1959.

18. Rockwell, Theodore, III. Reactor shielding design manual. Princeton, N. J., D. Van Nostrand Co., Inc. 1956.

19. Spinrad, B. I. and Kurath, Dieter. Computation forms for solution of critical problems by two-group diffusion theory. U. S. Atomic Energy Commission Report ANL-4352 [Argonne National Laboratory, Lemont, Ill.]. 1952.

20. Webster, J. W. An analysis of the accuracy of perturbation theory. U. S. Atomic Energy Commission Report IDO-16173 [Idaho Operations Office, AEC]. 1954.

21. Weinberg, Alvin M. and Wigner, Eugene P. The physical theory of neutron chain reactors. Chicago, Ill., The University of Chicago Press. 1958.

ACKNOWLEDGMENTS

The author wishes to express sincere appreciation to Dr. Glenn Murphy, Head of the Department of Nuclear Engineering, for his guidance, assistance, and encouragement in the formulation, development, and completion of this dissertation.